Downloaded from http://www.jci.org on March 11, 2015. http://dx.doi.org/10.1172/JCI74747

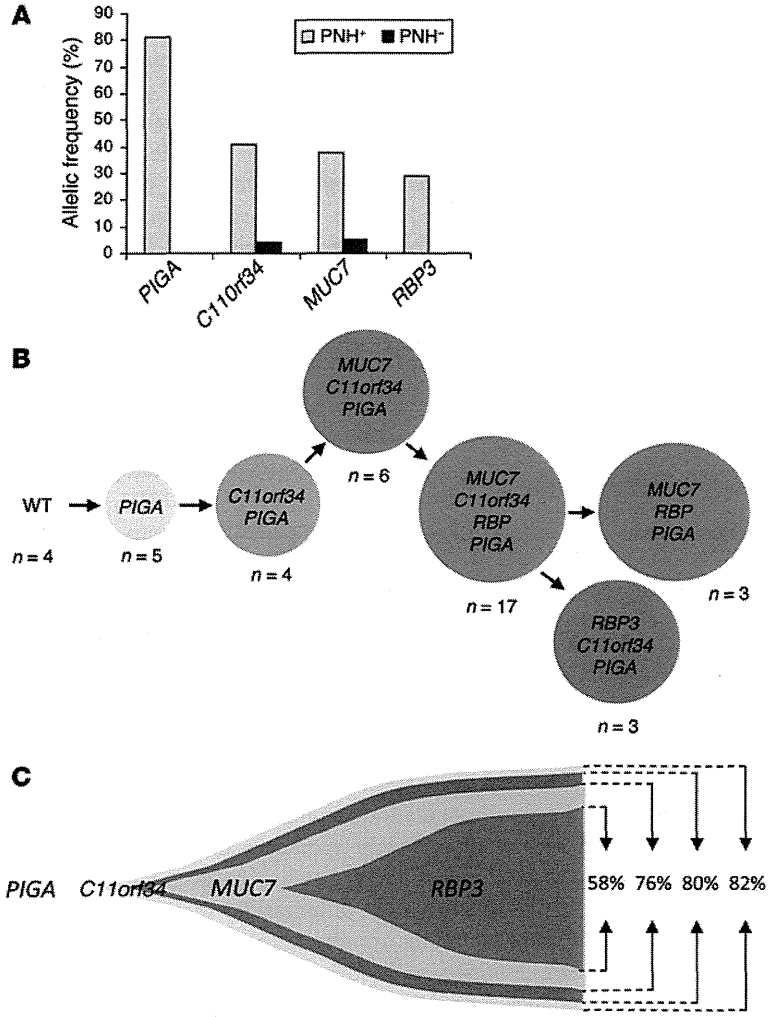

Figure 3. *PIGA* mutation as the initial ancestral event in PNH8. (**A**) A *PIGA* mutation together with 3 other somatic mutations (*C11orf34*, *RBP3*, and *MUC7*) were detected via WES at various allelic frequencies. All mutations were confined to the PNH fraction. Of note is that, in this case, the *PIGA* mutation was hemizygous, rendering the clone size equivalent to the allelic frequency. (**B**) Single-colony Sanger sequencing further confirmed the results obtained from deep sequencing and suggested that a *PIGA* mutation was the initial event. *n* = the number of colonies with the indicated mutations observed. Colonies that were not reproducible in independent experiments are not shown. (**C**) Proposed model of clonal architecture in this case based on VAFs and colony sequencing results.

tissue to clarify the mutational spectrum in PNH, as it is possible that some pre-*PIGA* mutations were excluded due to their presence in the entire hematopoietic compartment.

Our study, while showing that intrinsic somatic factors may contribute to clonal expansion, is also consistent with the immune selection theory of the evolution of PNH. Multiple independent clones characterized by *PIGA* mutations illustrate that a growth advantage may promote selection of several privileged clones, which in the process of disease may be further enabled by subsequent somatic events or by primordial passenger events in the ancestral stem cell affected by *PIGA* mutations. Phenotypically, this intraclonal diversity may not be easily distinguishable, although we have identified a significant relationship between the presence of both type II and type III PNH cells in patients with more than 1 *PIGA* mutation, supporting previous research (40). Nevertheless, our results suggest that deep targeted NGS of *PIGA* may have ancillary diagnostic potential in PNH, including quantitating the clonal size and composition of aberrant cells, yet flow cytometry remains the most effective diagnostic method, as we failed to detect *PIGA* mutations in 3 of 12 cases by WES, 1 of 10 by targeted deep sequencing, and 21 of 36 by Sanger sequencing. Other genes in the biosynthetic pathway, including all other PIG genes such as *PIGT* (41), were examined in WES cases, but no lesions were found, raising the possibility that intronic mutations may lead to the loss of GPI anchors on the cell surface. Furthermore, the high failure rate of Sanger sequencing could be due to a number of reasons including small clone size, intronic mutations, or micro/large deletions only detectable by SNP array.

At the onset of our study, we postulated several theoretical possibilities as to the clonal architecture of PNH: (a) *PIGA* gene defects are the initial ancestral events, and other mutations are acquired subsequently, similar to the situation in MDS; (b) other initial somatic events are followed by *PIGA* mutations constrained within and completely overlapping the PNH clone, suggesting that the initial non-*PIGA* events are passenger mutations; (c) secondary *PIGA* mutations arise in the context of other clonogenic mutations that are present in both *PIGA* mutant and wild-type cells; and (d) both myelodysplastic and PNH clones independently coexist. While *PIGA* mutations appear to be the initial event in many cases, we identified concomitant somatic mutations in a large proportion of PNH patients. In such cases, subsequent subclonal events can occur and are similar to those present in more aggressive hematologic malignancies. In cases in which the preceding clonal mutation was found but was limited to the PNH fraction, one could suggest that a passenger mutation was clonally "fixed" by the subsequent *PIGA* event. However, in some cases, permissive leukemogenic effects appeared to be instigated by mutations in *JAK2*, *TET2*, or *STAC3*, suggesting that these primary events arose, conveying an initial growth advantage, with a *PIGA* mutation as a subclone conveying an additional growth advantage. In particular, the presence of 2 cases with "myeloproliferative" *JAK2* mutations suggests that the propensity toward clonal proliferation may be further modified by the presence of *PIGA* defects and that *JAK2* mutations in concert with *PIGA* mutations lead to a markedly different phenotype than that of a myeloproliferative neoplasm (MPN). In addition, there were a significant number of cases in which *PIGA* was the lone mutation, although WES data suggest that this may be less frequent when entire exomes are analyzed.

Regardless, in many cases, the subclonal or clonal occurrence of associated mutations resembles the typical architecture of MDS (10). We and others have previously described additional somatic events in PNH patients demonstrating that even *PIGA*

Downloaded from http://www.jci.org on March 11, 2015. http://dx.doi.org/10.1172/JCI74747

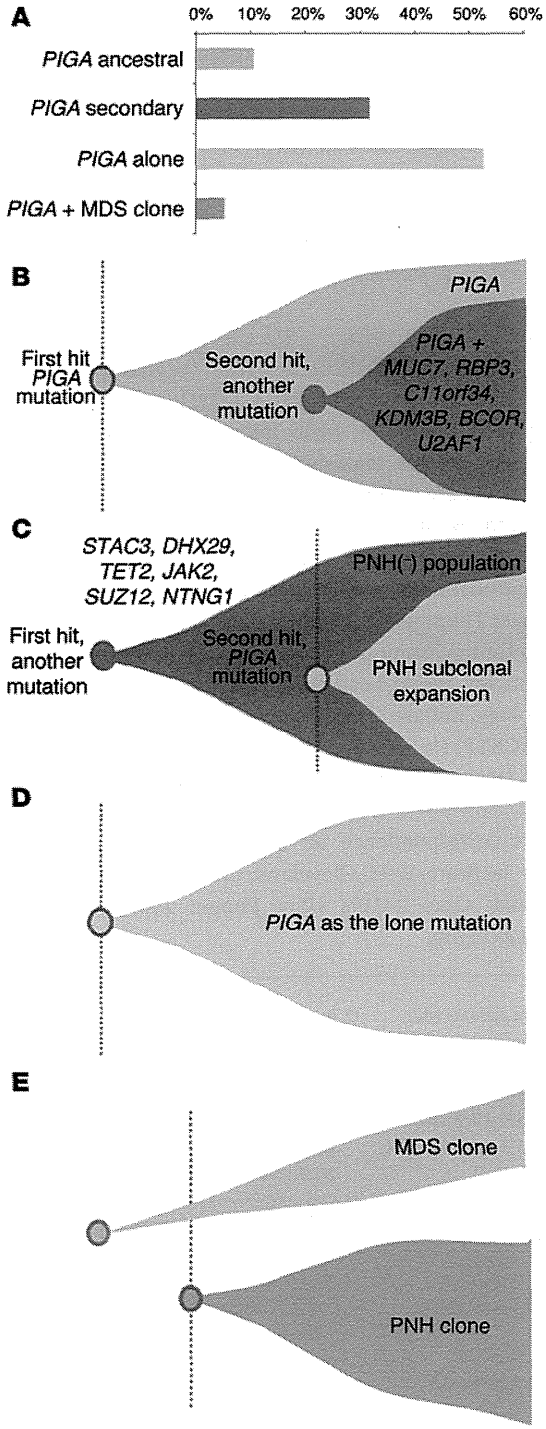

Figure 4. Mutational summary and clonal architecture scenarios. (A) Cohort frequency of 4 different scenarios for the clonal architecture encountered in PNH: ancestral *PIGA* mutation (**B**), secondary *PIGA* mutation (**C**), *PIGA* mutation as an isolated genetic event (**D**), and *PIGA* mutation leading to a PNH clone that independently coexists with an MDS clone (**E**).

mutation–negative cases were clonal (6–8). The inability to detect significant recurrent additional mutations may be due to the relatively small cohort and surprising diversity discovered in this study. Nevertheless, our results suggest that an obligatory secondary event does not occur in PNH, yet PNH clonal expansions appear to be aided by the presence of additional mutations. Depending on the permissivity of additional genetic events, the *PIGA* mutant clone may expand quickly, smolder, or disappear. This heterogeneous scenario would also be consistent with a relative lack of correlation between immunosuppression and the size of the clone, which may be driven under some circumstances by additional subclonal events. Our results suggest that future investigations into PNH will offer the opportunity to examine the implications of hematopoiesis sustained primarily by 1 or 2 mutated stem cells, with many cases demonstrating an accumulation of additional mutations that may be due to an increase in the self-renewal burden placed on stem cells as a consequence of the disease.

Methods

Patients. Bone marrow aspirates and/or blood samples were collected from 60 patients with PNH at the Cleveland Clinic. Diagnosis was confirmed and assigned according to the guidelines for the diagnosis and management of PNH (42).

Cytogenetics and SNP arrays. Cytogenetic analysis was performed according to standard banding techniques based on 20 metaphases, if available. Technical details regarding sample processing for SNP array (SNP-A) assays were previously described (43, 44). Affymetrix 250K and 6.0 kits were used. A stringent algorithm was applied for the identification of SNP-A lesions. Patients with SNP-A lesions concordant with metaphase cytogenetics or typical lesions known to be recurrent required no further analysis. Changes reported in our internal or publicly available (Database of Genomic Variants; http://projects.tcag.ca/variation) copy number variation (CNV) databases were considered nonsomatic and excluded. Results were analyzed using CNAG version 3.0 (20) or Genotyping Console (Affymetrix). All other lesions were confirmed as somatic or germline by analysis of CD3-sorted cells (45).

WES. WES was performed as previously reported (46). Briefly, tumor DNA was extracted from patients' bone marrow or peripheral blood mononuclear cells. DNA was obtained from paired CD59-positive and -negative cells. Whole-exome capture was accomplished based on liquid-phase hybridization (SureSelect; Agilent Technologies) according to the manufacturer's protocol. The SureSelect Human All Exon 50 Mb kit was used for 12 cases. The captured targets were subjected to massive sequencing using Illumina HiSeq 2000 according to the manufacturer's instructions. The raw sequence data were processed through the in-house pipeline constructed for whole-exome analysis of paired cancer genomes at the Human Genome Center, Institute of Medical Science, The University of Tokyo, and are summarized in a previous report (46). Data processing was divided into 2 steps: (a) generation of a BAM file (http://samtools.sourceforge.net/) for paired normal and tumor samples for each case, and (b) detection of somatic SNVs and indels by comparing normal and tumor BAM files. Alignment of sequencing reads on hg19 was visualized using Integrative Genomics Viewer (IGV) software (http://www.broadinstitute.org/igv/) (47).

Targeted deep sequencing and Sanger sequencing. We applied targeted exon sequencing to the validation of WES results as previously described (46, 48). Briefly, the number of reads containing SNVs and indels in both tumor and reference samples was determined using SAM tools, and the null hypothesis of equal allele frequencies in PNH and non-PNH samples was tested using the 2-tailed Fisher's exact test. A variant was adopted as a candidate somatic mutation if it had a *P* value

Downloaded from http://www.jci.org on March 11, 2015. http://dx.doi.org/10.1172/JCI74747

of less than 0.01. First, amplicons of each observation were subjected to Sanger sequencing by standard techniques on an ABI 3730xl DNA analyzer (Applied Biosystems). All mutations were confirmed by bidirectional sequencing and scored as pathogenic if not present in nonclonal, paired CD59-derived DNA. Then, deep NGS was applied to additional validation for variant allelic frequency and small clone detections. The amplicon libraries were generated according to an Illumina pair-end library protocol and subjected to deep sequencing on an Illumina MiSeq sequencer according to the standard protocol. For *PIGA* (exons 2–6) and *KDM3B* (exons 1–24), direct genomic sequencing was performed as previously described, together with deep sequencing, so that even very small mutated events would not be missed.

Single-cell colony culture. Colony formation assays in semi-solid cultures were used to obtain colonies for single-colony sequencing. A total of 10^5 bone marrow cells from PNH patients were plated in 1 ml of methylcellulose supplemented with G-SCF, GM-SCF, and EPO cytokines (STEMCELL Technologies) as well as FBS in a 35-mm culture plate at 37°C with 5% CO_2. After 7 to 10 days of culturing, individual colonies were removed, and DNA was extracted for sequencing.

Cell sorting. Following lysis of rbc, immunomagnetic selection of cells was performed using anti-CD59 PE (Life Technologies) followed by anti-PE microbeads (Miltenyi Biotec). Samples were separated using LS Columns (Miltenyi Biotec), and purity was verified in each fraction by flow cytometry on a Beckman Coulter FC500.

Flow cytometry. Whole blood was stained with antibodies against GlyA, CD15, CD24, CD55, CD59 (Beckman Coulter), CD59 (Life Technologies), and FLAER (Alexa 488 Proaerolysin Variant; Cedarlane Scientific) in various combinations to quantitate the number of GPI-deficient rbc and wbc in each patient. Samples were run on a Beckman Coulter FC500 or XL-MCL.

Accession codes. WES results have been deposited in the Sequence Read Archive (SRA) public database (PRJNA254174).

Statistics. JMP Pro 10 (SAS Institute Inc.) was used for statistical analysis. Either a Wilcoxon or Fisher's exact test was performed to evaluate statistically significant differences between groups, with an α of 0.05.

Study approval. Research was conducted according to protocols approved by the IRB of the Cleveland Clinic and in accordance with Declaration of Helsinki principles. Written informed consent was received from all patients prior to enrollment in the study.

Acknowledgments

This work was supported by grants from the NIH (RO1HL-082983, U54 RR019391, and K24 HL-077522, to J.P. Maciejewski); the Aplastic Anemia & MDS International Foundation (to J.P. Maciejewski and H. Makishima); the Robert Duggan Charitable Fund (to J.P. Maciejewski); Scott Hamilton CARES (to H. Makishima); the Ministry of Health, Labor and Welfare of Japan and KAKENHI (grants-in-aid 23249052, 22134006, and 21790907, to S. Ogawa); the Project for Development of Innovative Research on Cancer Therapeutics (P-DIRECT) (to S. Ogawa); and the Japan Society for the Promotion of Science (JSPS) through the Funding Program for World-Leading Innovative R&D on Science and Technology, initiated by the Council for Science and Technology Policy (CSTP) (to S. Ogawa). W. Shen was partly supported by the Jiangsu Health International Exchange Program (China).

Address correspondence to: Jaroslaw P. Maciejewski, Taussig Cancer Institute/R40, Cleveland Clinic, 9500 Euclid Avenue, Cleveland, Ohio 44195, USA. Phone: 216.445.5962; E-mail: maciejj@ccf.org.

1. Brodsky RA. Paroxysmal nocturnal hemoglobinuria: stem cells and clonality. *Hematology Am Soc Hematol Educ Program.* 2008;111–115.
2. Takeda J, et al. Deficiency of the GPI anchor caused by a somatic mutation of the PIG-A gene in paroxysmal nocturnal hemoglobinuria. *Cell.* 1993;73(4):703–711.
3. Young NS, Calado RT, Scheinberg P. Current concepts in the pathophysiology and treatment of aplastic anemia. *Blood.* 2006;108(8):2509–2519.
4. Maciejewski JP, Sloand EM, Sato T, Anderson S, Young NS. Impaired hematopoiesis in paroxysmal nocturnal hemoglobinuria/aplastic anemia is not associated with a selective proliferative defect in the glycosylphosphatidylinositol-anchored protein-deficient clone. *Blood.* 1997;89(4):1173–1181.
5. Araten DJ, Nafa K, Pakdeesuwan K, Luzzatto L. Clonal populations of hematopoietic cells with paroxysmal nocturnal hemoglobinuria genotype and phenotype are present in normal individuals. *Proc Natl Acad Sci U S A.* 1999;96(9):5209–5214.
6. Inoue N, et al. Molecular basis of clonal expansion of hematopoiesis in 2 patients with paroxysmal nocturnal hemoglobinuria (PNH). *Blood.* 2006;108(13):4232–4236.
7. O'Keefe CL, et al. Deletions of Xp22.2 including PIG-A locus lead to paroxysmal nocturnal hemoglobinuria. *Leukemia.* 2011;25(2):379–382.
8. Mortazavi Y, Tooze JA, Gordon-Smith EC, Rutherford TR. N-RAS gene mutation in patients with aplastic anemia and aplastic anemia/ paroxysmal nocturnal hemoglobinuria during evolution to clonal disease. *Blood.* 2000;95(2):646–650.
9. Sugimori C, et al. Paroxysmal nocturnal hemoglobinuria and concurrent JAK2(V617F) mutation. *Blood Cancer J.* 2012;2(3):e63.
10. Walter MJ, et al. Clonal architecture of secondary acute myeloid leukemia. *N Engl J Med.* 2012;366(12):1090–1098.
11. Ley TJ, et al. DNA sequencing of a cytogenetically normal acute myeloid leukaemia genome. *Nature.* 2008;456(7218):66–72.
12. Bessler M, Mason P, Hillmen P, Luzzatto L. omatic mutations and cellular selection in paroxysmal nocturnal haemoglobinuria. *Lancet.* 1994;343(8903):951–953.
13. Mazelin L, et al. Netrin-1 controls colorectal tumorigenesis by regulating apoptosis. *Nature.* 2004;431(7004):80–84.
14. Arakawa H. Netrin-1 and its receptors in tumorigenesis. *Nat Rev Cancer.* 2004;4(12):978–987.
15. van Gils JM, et al. The neuroimmune guidance cue netrin-1 promotes atherosclerosis by inhibiting the emigration of macrophages from plaques. *Nat Immunol.* 2012;13(2):136–143.
16. Cavard C, et al. Gene expression profiling provides insights into the pathways involved in solid pseudopapillary neoplasm of the pancreas. *J Pathol.* 2009;218(2):201–209.
17. Burrell RA, McGranahan N, Bartek J, Swanton C. The causes and consequences of genetic heterogeneity in cancer evolution. *Nature.* 2013;501(7467):338–345.
18. Meacham CE, Morrison SJ. Tumour heterogeneity and cancer cell plasticity. *Nature.* 2013;501(7467):328–337.
19. Cancer Genome Atlas Research Network. Comprehensive genomic characterization defines human glioblastoma genes and core pathways. *Nature.* 2008;455(7216):1061–1068.
20. Cancer Genome Atlas Research Network. Genomic and epigenomic landscapes of adult de novo acute myeloid leukemia. *N Engl J Med.* 2013;368(22):2059–2074.
21. Stransky N, et al. The mutational landscape of head and neck squamous cell carcinoma. *Science.* 2011;333(6046):1157–1160.
22. Graubert TA, et al. Recurrent mutations in the U2AF1 splicing factor in myelodysplastic syndromes. *Nat Genet.* 2011;44(1):53–57.
23. Makishima H, et al. Mutations in the spliceosome machinery, a novel and ubiquitous pathway in leukemogenesis. *Blood.* 2012;119(14):3203–3210.
24. Ko M, et al. Impaired hydroxylation of 5-methylcytosine in myeloid cancers with mutant TET2. *Nature.* 2010;468(7325):839–843.
25. Koh SS, et al. Differential gene expression profiling of primary cutaneous melanoma and sentinel lymph node metastases. *Mod Pathol.*

Downloaded from http://www.jci.org on March 11, 2015. http://dx.doi.org/10.1172/JCI74747

2012;25(6):828–837.
26. Shima H, et al. Bromodomain-PHD finger protein 1 is critical for leukemogenesis associated with MOZ-TIF2 fusion. *Int J Hematol.* 2014; 99(1):21–31.
27. Sun HT, Cheng SX, Tu Y, Li XH, Zhang S. FoxQ1 promotes glioma cells proliferation and migration by regulating NRXN3 expression. *PLoS One.* 2013;8(1):e55693.
28. Kim JY, et al. KDM3B is the H3K9 demethylase involved in transcriptional activation of lmo2 in leukemia. *Mol Cell Biol.* 2012;32(14):2917–2933.
29. Liu L, Sanchez-Bonilla M, Crouthamel M, Giachelli C, Keel S. Mice lacking the sodium-dependent phosphate import protein, PiT1 (SLC20A1), have a severe defect in terminal erythroid differentiation and early B cell development. *Exp Hematol.* 2013;41(5):432–443.
30. Byrd JC, Bresalier RS. Mucins and mucin binding proteins in colorectal cancer. *Cancer Metastasis Rev.* 2004;23(1–2):77–99.
31. Cheung KJ, et al. High resolution analysis of follicular lymphoma genomes reveals somatic recurrent sites of copy-neutral loss of heterozygosity and copy number alterations that target single genes. *Genes Chromosomes Cancer.* 2010;49(8):669–681.
32. Summers KM, et al. Experimental and bioinformatic characterisation of the promoter region of the Marfan syndrome gene, FBN1. *Genomics.* 2009;94(4):233–240.
33. Liu C, et al. SUZ12 is involved in progression of non-small cell lung cancer by promoting cell proliferation metastasis. *Tumour Biol.* 2014;35(6):6073–6082.
34. Abdel-Wahab O, Dey A. The ASXL-BAP1 axis: new factors in myelopoiesis, cancer and epigenetics. *Leukemia.* 2013;27(1):10–15.
35. Panagopoulos I, et al. Fusion of the ZC3H7B and BCOR genes in endometrial stromal sarcomas carrying an X;22-translocation. *Genes Chromosomes Cancer.* 2013;52(7):610–618.
36. Parsyan A, et al. The helicase protein DHX29 promotes translation initiation, cell proliferation, and tumorigenesis. *Proc Natl Acad Sci U S A.* 2009;106(52):22217–22222.
37. Roy S, et al. BCR-ABL1 tyrosine kinase sustained MECOM expression in chronic myeloid leukaemia. *Br J Haematol.* 2012;157(4):446–456.
38. Gomez-Segui I, et al. Novel recurrent mutations in the RAS-like GTP-binding gene RIT1 in myeloid malignancies. *Leukemia.* 2013; 27(9):1943–1946.
39. Kralovics R, et al. A gain-of-function mutation of JAK2 in myeloproliferative disorders. *N Engl J Med.* 2005;352(17):1779–1790.
40. Rollinson S, Richards S, Norfolk D, Bibi K, Morgan G, Hillmen P. Both paroxysmal nocturnal hemoglobinuria (PNH) type II cells and PNH type III cells can arise from different point mutations involving the same codon of the PIG-A gene. *Blood.* 1997;89(8):3069–3071.
41. Krawitz PM, et al. A case of paroxysmal nocturnal hemoglobinuria caused by a germline mutation and a somatic mutation in PIGT. *Blood.* 2013;122(7):1312–1315.
42. Parker C, et al. Diagnosis and management of paroxysmal nocturnal hemoglobinuria. *Blood.* 2005;106(12):3699–3709.
43. Maciejewski JP, Tiu RV, O'Keefe C. Application of array-based whole genome scanning technologies as a cytogenetic tool in haematological malignancies. *Br J Haematol.* 2009;146(5):479–488.
44. Gondek LP, et al. Chromosomal lesions and uniparental disomy detected by SNP arrays in MDS, MDS/MPD, and MDS-derived AML. *Blood.* 2008;111(3):1534–1542.
45. Tiu RV, et al. New lesions detected by single nucleotide polymorphism array-based chromosomal analysis have important clinical impact in acute myeloid leukemia. *J Clin Oncol.* 2009;27(31):5219–5226.
46. Yoshida K, et al. Frequent pathway mutations of splicing machinery in myelodysplasia. *Nature.* 2011;478(7367):64–69.
47. Robinson JT, et al. Integrative genomics viewer. *Nat Biotechnol.* 2011;29(1):24–26.
48. Makishima H, et al. Somatic SETBP1 mutations in myeloid malignancies. *Nat Genet.* 2013;45(8):942–946.

European Journal of Haematology

European Journal of Haematology

ORIGINAL ARTICLE

Increased glycosylphosphatidylinositol-anchored protein-deficient granulocytes define a benign subset of bone marrow failures in patients with trisomy 8

Kohei Hosokawa[1]*, Naomi Sugimori[1]*, Takamasa Katagiri[2], Yumi Sasaki[1], Chizuru Saito[1], Yu Seiki[1], Kanako Mochizuki[1], Hirohito Yamazaki[1], Akiyoshi Takami[1], Shinji Nakao[1]

[1]Cellular Transplantation Biology, Kanazawa University Graduate School of Medical Science, Kanazawa; [2]Clinical Laboratory Science, Kanazawa University Graduate School of Medical Science, Kanazawa, Japan

Abstract

Trisomy 8 (+8), one of the most common chromosomal abnormalities found in patients with myelodysplastic syndromes (MDS), is occasionally seen in patients with otherwise typical aplastic anemia (AA). Although some studies have indicated that the presence of +8 is associated with the immune pathophysiology of bone marrow (BM) failure, its pathophysiology may be heterogeneous. We studied 53 patients (22 with AA and 31 with low-risk MDS) with +8 for the presence of increased glycosylphosphatidylinositol-anchored protein-deficient (GPI-AP$^-$) cells, their response to immunosuppressive therapy (IST), and their prognosis. A significant increase in the percentage of GPI-AP$^-$ cells was found in 14 (26%) of the 53 patients. Of the 26 patients who received IST, including nine with increased GPI-AP$^-$ cells and 17 without increased GPI-AP$^-$ cells, 14 (88% with increased GPI-AP$^-$ cells and 41% without increased GPI-AP$^-$ cells) improved. The overall and event-free survival rates of the +8 patients with and without increased GPI-AP$^-$ cells at 5 yr were 100% and 100% and 59% and 57%, respectively. Examining the peripheral blood for the presence of increased GPI-AP$^-$ cells may thus be helpful for choosing the optimal treatment for +8 patients with AA or low-risk MDS.

Key words trisomy 8; bone marrow failure; GPI-AP$^-$ cells; immunosuppressive therapy

Correspondence Shinji Nakao, MD, PhD, Cellular Transplantation Biology, Kanazawa University Graduate School of Medical Science, 13-1 Takaramachi, Kanazawa, Ishikawa 920-8640, Japan. Tel: 81-76-265-2274; Fax: 81-76-234-4252; e-mail: snakao8205@staff.kanazawa-u.ac.jp

*KH and NS contributed equally to this manuscript.

Accepted for publication 13 November 2014

doi:10.1111/ejh.12484

Karyotypic abnormalities in patients with bone marrow failure are generally regarded as a hallmark of clonal hematopoietic disorders with the propensity toward transformation into acute myeloid leukemia (AML). The incidence of cytogenetic abnormalities in aplastic anemia (AA) and myelodysplastic syndromes (MDS) is approximately 4% and 50%, respectively (1, 2). Trisomy 8 (+8), one of the most frequent chromosomal abnormalities found in patients with MDS, is occasionally seen in patients with otherwise typical AA (3–8). A recent study based on 2072 MDS patients showed that 8% of these patients had +8 in isolation (9). For both AML and MDS, +8 is listed in the 'intermediate-risk cytogenetic group' (6, 9, 10). Several studies have shown that MDS patients with +8 are highly responsive to immunosuppressive therapy (IST) (3, 7, 11). However, +8 in AA patients is associated with an increased risk of evolving into MDS/AML (5, 8). Thus, the prognostic significance of +8 in patients with AA or low-risk MDS remains unclear.

Small populations of glycosylphosphatidylinositol-anchored protein-deficient (GPI-AP$^-$) blood cells are often detected in the peripheral blood (PB) of patients with AA or low-risk MDS, such as refractory anemia (RA) and refractory cytopenia with multilineage dysplasia (RCMD) in the FAB classification (12–14). The GPI-AP$^-$ blood cells are detectable even in patients with BM failure who have chromosomal abnormalities, including +8 (15–17). Parlier and Longo

© 2014 John Wiley & Sons A/S. Published by John Wiley & Sons Ltd

reported the first patient with GPI-AP$^-$ blood cells and + 8 who had ringed sideroblasts (18, 19). Our recent study showed a close association of del(13q) with the presence of increased GPI-AP$^-$ cells as well as a favorable response to immunosuppressive therapy (IST) (16). In patients with AA or RA possessing +8, the presence of GPI-AP$^-$ cells may affect response to IST as well as prognosis. To test this hypothesis, we analyzed clinical data of 53 BM failure patients with +8 whose blood cells were examined for the presence of GPI-AP$^-$ cells.

Patients and methods

Patients

This study included retrospective analysis of clinical records for 1228 BM failure patients: 733 with AA and 495 with low-risk MDS, including 286 with refractory cytopenia with unilineage dysplasia (RCUD), 149 with RCMD, and 60 with unclassified MDS (MDS-U). In all patients, blood samples were examined for the presence of GPI-AP$^-$ granulocytes and erythrocytes at our laboratory between May 1999 and July 2010. BM smear slides and trephine biopsy specimens were reviewed by two independent hematologists. BM cellularity was expressed as the percentage of BM volume occupied by hematopoietic cells in the trephine biopsy specimens. Hypocellular marrow was defined as <30% cellularity in patients <70 yr, or <20% cellularity in patients ≥70 yr (20). Chromosomal analysis was conducted using the G-banding method, and the presence of +8 clones was confirmed by fluorescent *in situ* hybridization (FISH) when the number of +8 revealed by G-banding was less than or equal to two. The results of G-banding were described according to the International System for Human Cytogenetic Nomenclature (ISCN) (21). The Ethics Committee of Kanazawa University Graduate School of Medical Science approved the study protocol, and all patients provided informed consent prior to sampling.

Therapy and response criteria

Horse anti-thymocyte globulin (ATG, Lymphoglobulin, Genzyme, Cambridge, MA, USA) in combination with cyclosporine (CsA) was given to patients with severe aplastic anemia (SAA). Four to 6 mg/kg of CsA was administered to patients with moderate AA (MAA) or MDS. Trough levels of CsA were maintained between 150 and 250 ng/mL. Six patients (four with AA and two with MDS) received 10–20 mg/d of methenolone acetate in addition to CsA. Responses to IST were defined according to the established criteria (22, 23).

Monoclonal antibodies

Monoclonal antibodies (mAbs) used for flow cytometry were FITC-conjugated anti-CD59 (P282E, IgG2a; Beckman Coulter, Brea, CA, USA), FITC-conjugated anti-CD55 (IA10, IgG2a; BD PharMingen, San Diego, CA, USA), PE-conjugated anti-CD11b/Mac-1 (ICRF44, IgG1; BD PharMingen), and PE-conjugated anti-glycophorin A (JC159, IgG1; Dako, Glostrup, Denmark).

Detection of GPI-AP$^-$ cells by flow cytometry

All blood samples were analyzed within 24 h of collection to avoid false-positive results due to cell damage. Staining with each mAb was performed according to the lyse-stain protocol as previously described (24, 25). The presence of CD55$^-$CD59$^-$glycophorin A$^+$ erythrocytes at the level of ≥0.005% and/or CD55$^-$CD59$^-$CD11b$^+$ granulocytes at the level of ≥0.003% was defined as an abnormal increase ('positive') based on results obtained from 183 healthy individuals (26). With careful handling of samples and elaborate gating strategies, cutoff values can be lowered to these levels without producing false-positive results (24, 27, 28).

Statistical analysis

Prevalence of increased GPI-AP$^-$ cells among different patient populations was compared using the chi-squared test. The Kaplan–Meier method and the Cox proportional hazards model were used to estimate time-to-event analysis. Overall survival (OS) was calculated in months from date of diagnosis until date of death or last follow-up. Event-free survival (EFS) was defined as the time from diagnosis to AML evolution or death. Two-sided *P*-values were calculated, and $P < 0.05$ was considered statistically significant. All statistical analyses were carried out using the EZR software package (Saitama Medical Center, Jichi Medical University), a graphical user interface for R (The R Foundation for Statistical Computing, version 2.13.0) (29).

Results

Incidence of BM failure patients with +8

Of 754 patients with AA, 22 (2.9%) possessed +8; instead, of 483 patients with low-risk MDS, 31 (6.4%) possessed +8. Their clinical features are summarized in Table 1. The median age of patients with +8 was 61, and BM was hypocellular in 32 patients, normocellular in 15, and hypercellular in six. Thirty-five patients had trisomy 8 alone (+8 alone), while 18 patients had additional chromosomal abnormalities (+8 others). The median percentage of +8 cells in karyotyped cells was 15%. Diagnoses of 31 MDS patients according to the 2008 WHO classification included nine patients with RCUD, 16 with RCMD, and six with MDS-U. None of the patients with +8 had ringed sideroblasts. All MDS patients were classified as Int-1 according to the International Prognostic Scoring System (IPSS).

© 2014 John Wiley & Sons A/S. Published by John Wiley & Sons Ltd

Table 1 Clinical features of bone marrow failure patients with trisomy 8

UPN	Age	Sex	Dx	Cellularity	IPSS	% of +8 cells	Other abnormalities	% GPI-AP$^-$ Granulocytes	% GPI-AP$^-$ Erythrocytes	GPI-AP$^-$ cells	Treatment	Response	Outcome	Cause of death	AML transformation
1	69	M	SAA	Hypo	NE	5	–	0.034	0.038	Positive	ATG+CsA	PR	Death	Infection	No
2	21	F	SAA	Hypo	NE	25	+	39.124	2.106	Positive	ATG+CsA	PR	Alive		No
3	50	F	SAA	Hypo	NE	15	–	0.002	0.026	Positive	ATG+CsA →BMT	NR	Alive		No
4	26	F	SAA	Hypo	NE	10	–	0	0	Negative	ATG+CsA	PR	Death	Infection	No
5	16	M	SAA	Hypo	NE	20	–	0	0	Negative	ATG+CsA →BMT	NR	Death	Infection	No
6	26	M	SAA	Hypo	NE	15	–	0	0	Negative	Allo-BMT	NA	Death	Infection	Yes
7	68	M	SAA	Hypo	NE	5	–	0.002	0.002	Negative	Allo-BMT	NA	Alive		Yes
8	46	F	SAA	Hypo	NE	55	+	0	0.004	Negative	CsA→ Allo-BMT	NR	Death	GVHD	Yes
9	66	F	MAA	Hypo	NE	10	–	0.007	0	Positive	CsA	PR	Death	Infection	No
10	61	M	MAA	Hypo	NE	10	–	6.201	8.657	Positive	CsA	PR	Alive		No
11	50	M	MAA	Hypo	NE	10	–	0.033	0.039	Positive	CsA+AS	PR	Alive		No
12	71	M	MAA	Hypo	NE	10	–	0.049	0.092	Positive	CsA+AS	PR	Alive		No
13	68	M	MAA	Hypo	NE	5	–	0.363	0.045	Positive	No treatment	NA	Alive		No
14	65	F	MAA	Hypo	NE	80	–	0.64	0.327	Positive	No treatment	NA	Alive		No
15	69	M	MAA	Hypo	NE	15	–	0	0.001	Negative	CsA	NR	Death	Lung cancer	No
16	35	M	MAA	Hypo	NE	5	–	0	0	Negative	CsA	NR	Alive		No
17	79	M	MAA	Hypo	NE	45	+	0	0	Negative	CsA	NR	Alive		No
18	71	F	MAA	Hypo	NE	30	–	0	0.002	Negative	CsA	PR	Alive		No
19	10	M	MAA	Hypo	NE	80	–	0	0.004	Negative	CsA+AS	NR	Death	Pneumonia	No
20	33	M	MAA	Hypo	NE	35	–	0	0	Negative	CsA+AS	PR	Alive		No
21	60	F	MAA	Hypo	NE	25	–	0	0.001	Negative	No treatment	NA	Alive		No
22	31	F	MAA	Hypo	NE	NE	–	0	0	Negative	No treatment	NA	Alive		No
23	42	F	RCUD(RA)	Normo	Int-1	50	+	0	0	Negative	CsA	NR	Death	Heart failure	No
24	87	F	RCUD(RA)	Hypo	Int-1	35	+	0	0.003	Negative	CsA+AS	NR	Death	Infection	No
25	70	M	RCUD(RA)	Hyper	Int-1	5	–	0	0	Negative	CsA+AS	NR	Death	Heart failure	No
26	81	M	RCUD(RA)	Normo	Int-1	5	+	0	0	Negative	AS,VitK	Progression	Death	Progression	No
27	51	M	RCUD(RA)	Hypo	Int-1	70	+	0	0	Negative	Allo-BMT	NA	Alive		No
28	56	F	RCUD(RA)	Normo	Int-1	85	–	0	0.001	Negative	PSL	SD	Alive		No

(continued)

© 2014 John Wiley & Sons A/S. Published by John Wiley & Sons Ltd

Table 1 (continued)

UPN	Age	Sex	Dx	Cellularity	IPSS	% of +8 cells	Other abnormalities	% GPI-AP$^-$ Granulocytes	% GPI-AP$^-$ Erythrocytes	GPI-AP$^-$ cells	Treatment	Response	Outcome	Cause of death	AML transformation
29	75	M	RCUD(RA)	Normo	Int-1	15	–	0	0.001	Negative	AS	Progression	Death	Progression	No
30	72	F	RCUD(RA)	Hypo	Int-1	75	+	0	0	Negative	No treatment	NA	Alive		No
31	66	F	RCUD(RA)	Normo	Int-1	10	+	0	0.01	Negative	No treatment	NA	Alive		No
32	81	M	RCMD	Hyper	Int-1	5	–	0.034	0	Positive	NA	NA	Alive		No
33	88	F	RCMD	Hyper	Int-1	50	–	0.142	0.23	Positive	AS	PR	Alive		No
34	18	F	RCMD	Hypo	Int-1	55	+	0.003	0.008	Positive	Allo-PBSCT	NA	Alive		No
35	59	F	RCMD	Hyper	Int-1	5	–	0.001	0.001	Negative	CsA	CR	Alive		No
36	65	M	RCMD	Hypo	Int-1	5	–	0	0.001	Negative	CsA	HI-1	Alive		No
37	28	F	RCMD	Normo	Int-1	20	–	0	0	Negative	CsA	HI-1	Alive		No
38	61	F	RCMD	Hyper	Int-1	100	–	0	0	Negative	CsA	HI-2	Death	Bleeding	No
39	59	M	RCMD	Hypo	Int-1	35	+	0.001	0.003	Negative	CsA	Progression	Death	Progression	Yes
40	51	F	RCMD	Hypo	Int-1	13	+	0	0.002	Negative	PSL	SD	Death	Infection	No
41	89	M	RCMD	Normo	Int-1	50	–	0	0	Negative	AraC	Progression	Death	Progression	No
42	72	M	RCMD	Normo	Int-1	10	+	0	0	Negative	VitK	NA	Death	Pneumonia	No
43	50	F	RCMD	Normo	Int-1	NE	–	0	0.001	Negative	AS,VitK	SD	Alive		No
44	77	F	RCMD	Normo	Int-1	10	+	0	0.003	Negative	AS	Progression	Death	Progression	Yes
45	7	M	RCMD	Normo	Int-1	10	–	0	0.002	Negative	Allo-BMT	NA	Death	TMA	No
46	63	F	RCMD	Normo	Int-1	NE	+	0	0	Negative	No treatment	NA	Death	Progression	No
47	56	F	RCMD	Normo	Int-1	40	–	0	0.002	Negative	No treatment	NA	Alive		No
48	70	F	MDS-U	Hypo	Int-1	5	+	0.005	0.023	Positive	CsA	CR	Alive		No
49	81	M	MDS-U	Hypo	Int-1	95	+	6.851	0.272	Positive	CsA	NA	Alive		No
50	75	M	MDS-U	Hyper	Int-1	5	–	0	0	Negative	AS	HI-3	Death	Infection	No
51	77	M	MDS-U	Normo	Int-1	35	+	0	0	Negative	AS,VitK	Progression	Death	Progression	No
52	34	F	MDS-U	Hypo	Int-1	NE	–	0	0	Negative	Allo-PBSCT	NA	Alive		No
53	55	F	MDS-U	Normo	Int-1	45	–	0	0	Negative	No treatment	NA	Alive		No
Median	61					15									

AML, acute myeloid leukemia; ATG, anti-thymocyte globulin; RCMD, refractory cytopenia with multilineage dysplasia; RCUD, refractory cytopenia with unilineage dysplasia; SAA, severe aplastic anemia.

© 2014 John Wiley & Sons A/S. Published by John Wiley & Sons Ltd

Prevalence of patients possessing increased GPI-AP$^-$ cells

As shown in Table 1, 14 (26.4%) of patients with +8 had GPI-AP$^-$ cells that accounted for 0.003% to 39.124% (median, 0.049%) of granulocytes. One patient who possessed 0.002% GPI-AP$^-$ granulocytes was judged positive because 0.026% of the patient's erythrocytes were GPI-AP$^-$ cells (Figure S1). None of the patients evolved into clinical PNH during the observation period of 2–10 yr. The prevalence of increased GPI-AP$^-$ cells was lower than that (43%) in 937 BM failure patients (637 with AA and 300 with MDS) with normal karyotype (16). Of 22 AA patients with +8, nine (41%) had increased GPI-AP$^-$ cells; instead, of 31 low-risk MDS patients with +8, five (16%) had increased GPI-AP$^-$ cells ($P = 0.04$).

Response to IST in BM failure patients with +8

Twenty-six patients (49%) were treated with IST, and 25 of these had evaluable responses. IST included CsA alone in 15 patients, CsA and ATG in five patients, and CsA and methenolone acetate in six patients. The overall response rate to IST in the +8 patients was 56% (14/25 patients). Of 16 AA patients with +8 treated with CsA and ATG (5) or CsA ± methenolone acetate (11), nine (56%) responded. Nine MDS patients with +8 were treated with CsA ± methenolone acetate, and five (56%) improved ($P = 0.97$). Of eight patients positive for GPI-AP$^-$ cells treated with IST, 7 (88%) responded; instead, of 17 patients negative for GPI-AP$^-$ cells, 7 (41%) responded ($P = 0.03$). Comparison of patients with +8 with 141 BM failure patients (120 with AA and 21 with MDS) with normal karyotypes that were included in our previous study (16) showed that +8 patients had lower response rates to IST than patients with normal karyotypes, 56% in +8 AA patients vs. 81% in normal karyotype AA patients ($P = 0.03$) and 56% in +8 MDS patients vs. 62% in normal karyotype MDS patients ($P = 0.75$), although the differences were not statistically significant in MDS patients (16).

Prognosis in BM failure patients with +8

None of the 14 + 8 patients with increased GPI-AP$^-$ cells progressed to advanced MDS or AML during the follow-up period of 2–239 months (median, 67 months). On the other hand, five of the 39 + 8 patients without GPI-AP$^-$ cells developed AML. The 5-yr OS and EFS rates of the 53 patients with +8 patients were 69.4% and 68.1%, respectively (Fig. 1A). The 5-yr OS/EFS rates of +8 patients with increased GPI-AP$^-$ cells were 100%/100%; instead, the 5-yr OS/EFS rates of +8 patients without increased GPI-AP$^-$ cells were 58.6%/56.9% ($P = 0.0347$, $P = 0.0269$, respectively; Fig. 1B). The 5-yr OS rates of +8 patients with +8 alone were 81.7%; instead, the 5-yr OS rates of +8 patients with +8 with other abnormalities were 45.5% ($P = 0.0196$; Fig. 1C). When age, gender, diagnosis, cellularity, clone size, karyotype complexity, and GPI-AP$^-$ cells were included in the multivariate analysis, higher age (60 yr or older) and the absence of GPI-AP$^-$ cells represented independent negative predictors for OS (Table 2).

To further evaluate the significance of GPI-AP$^-$ cells in +8 patients, the 5-yr OS rates of BM failure patients with +8 were compared with those of 246 BM failure patients (179 with AA and 67 with MDS) with normal karyotype who were included in our previous study (16). There was no significant difference in the survival rates between the two groups with increased GPI-AP$^-$ cells (100% vs. 92.7% $P = 0.914$; Fig. 2A), while the survival rate of +8 patients without increased GPI-AP$^-$ cells (58.6%) was lower than that of patients with normal karyotype not possessing increased GPI-AP$^-$ cells (79.5%, $P = 0.0007$; Fig. 2B).

Discussion

The current retrospective study of a large number of BM failure patients revealed distinctive clinical features of BM failure patients with +8 abnormalities. Of the 483 patients with low-risk MDS, 31 (6.6%) possessed +8, which was comparable to the 8% reported in a recent study of 2072 MDS patients (2). That study did not provide any detailed diagnoses of the patients with +8. The present study detected GPI-AP$^-$ cells in 26.4% of patients with +8, and the prevalence of increased GPI-AP$^-$ cell percentages was higher in AA patients (41%) than in those with low-risk MDS (16%). This study is the first to reveal the prevalence of increased GPI-AP$^-$ cell percentages based on a large number of AA and low-risk MDS patients with +8.

Approximately half of the patients with +8 were treated with IST, with an overall response rate of 56%. The relatively high response rate was probably achieved because IST was only administered to patients who had clinical features associated with a good response to IST, such as a short disease duration and the presence of thrombocytopenia with decreased megakaryocytes (30). The response rates were similar between AA (56%) and low-risk MDS patients (56%). However, there was a significant difference in the response rate between the patients with and those without increased GPI-AP$^-$ cells (88% vs. 41%).

Consistent with our current data, several studies demonstrated that AA and MDS patients with +8 are likely to respond to IST (3, 7, 11). There may thus be a common mechanism underlying the preferential commitment of hematopoietic progenitor clones with +8 in immune-mediated BM failures. One study revealed an increased expression of the WT1 gene by BM mononuclear cells from MDS patients with +8, which may elicit specific T-cell responses to WT1 peptides and lead to the suppression of non-+8 hematopoietic

© 2014 John Wiley & Sons A/S. Published by John Wiley & Sons Ltd

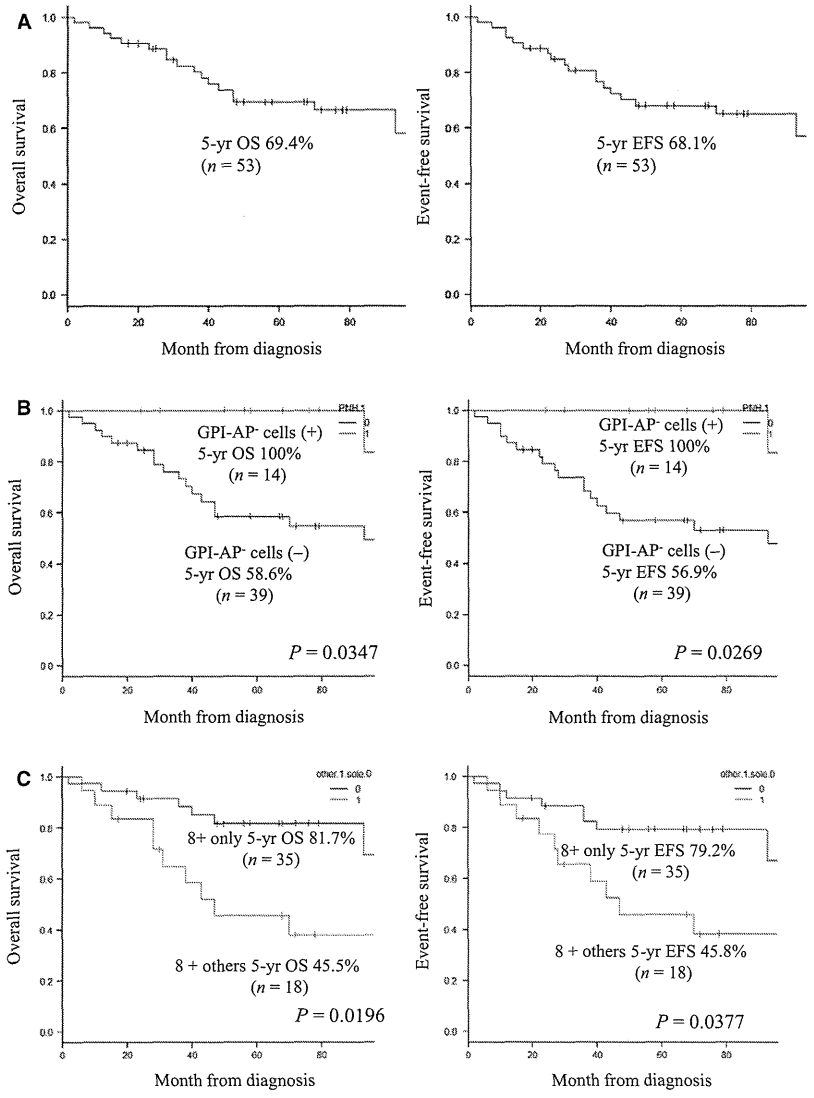

Figure 1 Overall and event-free survival rates of BM failure patients with trisomy 8. (A) Five-year overall survival (OS) and event-free survival (EFS) rates of +8 patients. (B) Five-year OS and EFS rates of +8 patients with and without increased GPI-AP$^-$ cells. (C) Five-year OS and EFS rates of +8 patients with +8 alone and +8 with other abnormalities (8+ others). The EFS was defined as the time from diagnosis to acute myeloid leukemia (AML) evolution or death.

Table 2 Results of multivariate analysis of prognostic factors for overall survival of patients with BM failure with trisomy 8

		BMF with trisomy 8	
Variable	Categories	Hazard ratio (95% CI)	*P*-value
Age	≥60 yr vs. <60 yr	3.9 (1.1–13.6)	<0.05
Sex	Male vs. female	1.5 (0.6–4.2)	0.42
Diagnosis	AA vs. MDS	1.3 (0.3–5.8)	0.74
Cellularity	Hypocellular vs. others	0.5 (0.1–1.9)	0.31
Karyotype complexity	8+ alone vs. 8+ others	0.4 (0.1–1.3)	0.12
Clone size (% of +8 cells)	≥15% vs. <15%	0.5 (0.2–1.3)	0.16
GPI-AP$^-$ cells	Positive vs. negative	0.1 (0.02–0.7)	<0.05

GPI-AP$^-$ cells, glycosylphosphatidylinositol-anchored protein-deficient blood cells; AA, aplastic anemia; MDS, myelodysplastic syndrome; CI, confidence interval; BMF, bone marrow failure.

progenitor cells by bystander effects of activated T cells (11). The same group proposed that BM CD34$^+$ cells of +8 patients exhibit resistance to apoptosis and increased myc expression as the mechanisms underlying the proliferative advantage of +8 clones (31). We were unable to examine WT1 gene expression and the number of WT1-specific T cells in our +8 patients

 © 2014 John Wiley & Sons A/S. Published by John Wiley & Sons Ltd

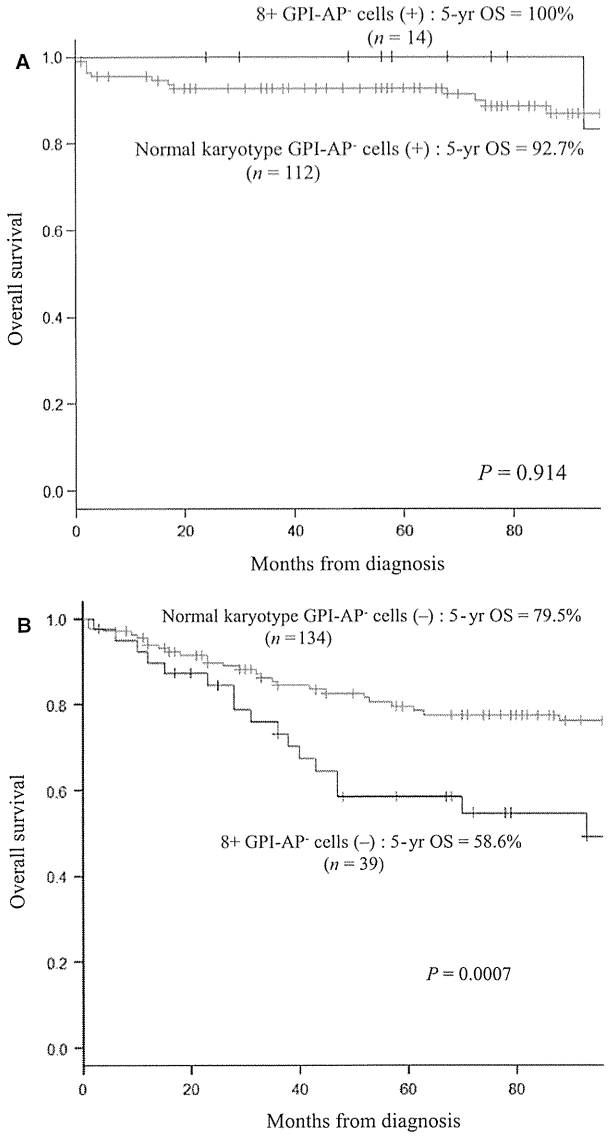

Figure 2 Overall survival rates of BM failure patients with trisomy 8 and normal karyotype. (A) Five-year overall survival (OS) rates of +8 patients and normal karyotype patients with increased GPI-AP$^-$ cells. (B) Five-year OS rates of +8 patients and normal karyotype patients without increased GPI-AP$^-$ cells.

who were responsive to IST. However, we believe that the specific immune responses to +8 clones may not be the main mechanism underlying the immune-mediated BM failure, for the following reasons: First, if the immune response is directed against +8 clones, successful T-cell suppression by IST should lead to the expansion of the abnormal clone. In reality, the changes in the percentage of +8 clones in patients responding to IST were highly variable and did not show a steady increase (Figure S2). Second, the likelihood of responding to IST was determined by the presence of GPI-AP$^-$ cells, not by the +8 clones; the +8 patients did not respond better to IST than patients with a normal karyotype (56% of AA patients with +8 vs. 81% of AA patients with a normal karyotype and 56% of MDS patients with +8 vs. 62% of MDS patients with a normal karyotype). Third, leukocytes with copy number-neutral loss of heterozygosity in the short arm of chromosome 6 (6pLOH) should be detected in patients with +8 if they are targets of cytotoxic T-cell attacks, based on our previous study showing that leukocytes with 6pLOH are detectable in 13% of AA patients (32). However, none of the six patients with +8 studied in the present population had leukocytes with 6pLOH (data not shown).

The IPSS classifies +8 as an intermediate risk factor for the progression of MDS (10, 33). The prognostic significance of +8 was confirmed by recent studies that involved MDS with at least 5% blasts (34). However, its significance in patients with AA and low-risk MDS with less than 5% blasts has not been extensively studied. In contrast to previous reports (3, 11), this study revealed that AA and MDS with less than 5% blasts comprise a subset of patients with a propensity to evolve into AML. Recently, Schanz *et al.* studied 2902 MDS patients including 133 patients with +8 who had a median blast percentage of 4% in their BM and revealed that the median overall survival of the 133 patients was 23 months (6). However, this study included 1190 (42.7%) patients with blast percentages >5% in the BM. The median overall survivals in our 53 patients with +8 were 78 months in AA and 43 months in MDS patients. This study is the first to estimate the overall survival in AA and low-risk MDS patients with +8 whose blast percentage in the BM is less than 5% based on a large number of patients.

On the other hand, the finding that the 5-yr EFS of +8 patients with an increased GPI-AP$^-$ cell percentage was 100% suggests that this subset of +8 BM failures is a benign type of BM failure similar to that of AA patients with normal karyotypes possessing increased GPI-AP$^-$ cells rather than a clonal disorder associated with a high risk of developing AML. The median age (66 yr vs. 59 yr) and prevalence of hypercellular marrow (14% vs. 10%) in patients with and without GPI-AP$^-$ cells were similar.

By comparing clinical courses between +8 patients and normal karyotype patients, both patient groups with increased GPI-AP$^-$ cells proved to have good prognosis regardless of the presence of +8, while in patients without increased GPI-AP$^-$ cells, the survival rate of +8 patients was significantly lower than that of patients with normal karyotype, strongly suggesting the importance of detecting GPI-AP$^-$ cells in predicting the prognosis of +8 patients. The WHO 2008 classification defined +8 as an intermediate-risk abnormality of MDS. The BM failure patients with +8 possessing an increased number of GPI-AP$^-$ cells may therefore be treated in an inappropriate way such as with hypomethylating agents and allogeneic stem cell transplantation from unrelated donors. Therefore, our present

© 2014 John Wiley & Sons A/S. Published by John Wiley & Sons Ltd

findings suggest that it is important to determine whether increased GPI-AP$^-$ cells are detectable when BM failure patients are found to have +8. The significance of detecting GPI-AP$^-$ cells in +8 patients needs to be confirmed by prospective studies involving a large number of BM failure patients.

Acknowledgements

The authors would like to thank Rie Ohmi for excellent technical assistance. We also thank the following physicians for providing patient data: Y. Terasaki of Toyama City Hospital, T. Yoshida and H. Kaya of Toyama Prefectural Central Hospital, H. Kimura of Northern Fukushima Medical Center, Y. Yonemura of Kumamoto University Hospital, M. Ueda and M. Yamaguchi of Ishikawa Prefectural Central Hospital, K. Usuki and K. Iijima of NTT Kanto Medical Center, T. Handa of Dokkyo Medical University Koshigaya Hospital, M. Hishizawa of Kyoto University Hospital, M. Nakaibayashi of Towada First Hospital, H. Kamezaki of Nagahama City Hospital, H. Kobayashi, N. Ichikawa, and I. Shimizu of Nagano Red Cross Hospital, M. Uoshima of Matsushita Memorial Hospital, T. Tamaki of Rinku General Medical Center, T. Hayashi of Hyogo Prefectural Amagasaki Hospital, S. Yamamoto of Sapporo City General Hospital, Y. Maeda of Okayama University Hospital, A. Matsuda of the Saitama International Medical Center, M. Inoue and M. Sato of Osaka Medical Center and the Research Institute for Maternal and Child Health, K. Uchimaru of the Institute of Medical Science at the University of Tokyo, K. Fujikawa of Chibaken Saiseikai Narashino Hospital, T. Morishita of Konan Kosei Hospital, H. Mihara of Aichi Medical University Hospital, J. Tanaka of Shimane University Hospital, M. Funaki of the Tokyo Metropolitan Tama Medical Center, H. Ogura of Maebashi Red Cross Hospital, J. Tanabe of Fujieda Municipal General Hospital, H. Ogasawara of Odate Municipal General Hospital, H. Sugawara of Sumitomo Hospital, K. Takenaka of Kyushu University Hospital, H. Kobayashi of Jichi Medical University Hospital, K. Sato of Suwa Red Cross Hospital, H. Sato of Saitama Red Cross Hospital, M. Fukazawa of Social Insurance Funabashi Central Hospital, and K. Kataoka of Tokyo University Hospital. This study was supported by grants awarded to S.N.

Authorship contributions

K.H. and N.S. contributed equally to this work and participated in designing and performing the research. K.H. conducted statistical analysis; N.S., T.K., Y.S., C.S, K.M., H.Y., and A.T. contributed patient samples and data; S.N. initiated and designed the study; K.H. wrote the manuscript with contributions from N.S. All authors critically reviewed the final manuscript.

Disclosure of conflict of interest

The authors report no potential conflict of interests.

References

1. Appelbaum FR, Barrall J, Storb R, Ramberg R, Doney K, Sale GE, Thomas ED. Clonal cytogenetic abnormalities in patients with otherwise typical aplastic anemia. *Exp Hematol* 1987;**15**:1134–9.
2. Haase D. Cytogenetic features in myelodysplastic syndromes. *Ann Hematol* 2008;**87**:515–26.
3. Maciejewski JP, Risitano A, Sloand EM, Nunez O, Young NS. Distinct clinical outcomes for cytogenetic abnormalities evolving from aplastic anemia. *Blood* 2002;**99**:3129–35.
4. Bernasconi P, Klersy C, Boni M, *et al.* World Health Organization classification in combination with cytogenetic markers improves the prognostic stratification of patients with de novo primary myelodysplastic syndromes. *Br J Haematol* 2007;**137**:193–205.
5. Kim SY, Lee JW, Lee SE, *et al.* The characteristics and clinical outcome of adult patients with aplastic anemia and abnormal cytogenetics at diagnosis. *Genes Chromosom Cancer* 2010;**49**:844–50.
6. Schanz J, Tuchler H, Sole F, *et al.* New comprehensive cytogenetic scoring system for primary myelodysplastic syndromes (MDS) and oligoblastic acute myeloid leukemia after MDS derived from an international database merge. *J Clin Oncol* 2012;**30**:820–9.
7. Gupta V, Brooker C, Tooze JA, Yi QL, Sage D, Turner D, Kangasabapathy P, Marsh JC. Clinical relevance of cytogenetic abnormalities at diagnosis of acquired aplastic anaemia in adults. *Br J Haematol* 2006;**134**:95–9.
8. Mikhailova N, Sessarego M, Fugazza G, *et al.* Cytogenetic abnormalities in patients with severe aplastic anemia. *Haematologica* 1996;**81**:418–22.
9. Haase D, Germing U, Schanz J, *et al.* New insights into the prognostic impact of the karyotype in MDS and correlation with subtypes: Evidence from a core dataset of 2124 patients. *Blood* 2007;**110**:4385–95.
10. Greenberg P, Cox C, LeBeau MM, *et al.* International scoring system for evaluating prognosis in myelodysplastic syndromes. *Blood* 1997;**89**:2079–88.
11. Sloand EM, Mainwaring L, Fuhrer M, Ramkissoon S, Risitano AM, Keyvanafar K, Lu J, Basu A, Barrett AJ, Young NS. Preferential suppression of trisomy 8 compared with normal hematopoietic cell growth by autologous lymphocytes in patients with trisomy 8 myelodysplastic syndrome. *Blood* 2005;**106**:841–51.
12. Dunn DE, Tanawattanacharoen P, Boccuni P, Nagakura S, Green SW, Kirby MR, Kumar MS, Rosenfeld S, Young NS. Paroxysmal nocturnal hemoglobinuria cells in patients with bone marrow failure syndromes. *Ann Intern Med* 1999;**131**:401–8.
13. Wang H, Chuhjo T, Yasue S, Omine M, Nakao S. Clinical significance of a minor population of paroxysmal nocturnal

 © 2014 John Wiley & Sons A/S. Published by John Wiley & Sons Ltd

hemoglobinuria-type cells in bone marrow failure syndrome. *Blood* 2002;**100**:3897–902.
14. Wang SA, Pozdnyakova O, Jorgensen JL, Medeiros LJ, Stachurski D, Anderson M, Raza A, Woda BA. Detection of paroxysmal nocturnal hemoglobinuria clones in patients with myelodysplastic syndromes and related bone marrow diseases, with emphasis on diagnostic pitfalls and caveats. *Haematologica* 2009;**94**:29–37.
15. Araten DJ, Swirsky D, Karadimitris A, *et al.* Cytogenetic and morphological abnormalities in paroxysmal nocturnal haemoglobinuria. *Br J Haematol* 2001;**115**:360–8.
16. Hosokawa K, Katagiri T, Sugimori N, Ishiyama K, Sasaki Y, Seiki Y, Sato-Otsubo A, Sanada M, Ogawa S, Nakao S. Favorable outcome of patients who have 13q deletion: a suggestion for revision of the WHO 'MDS-U' designation. *Haematologica* 2012;**97**:1845–1849.
17. Sloand EM, Fuhrer M, Keyvanfar K, Mainwaring L, Maciejewski J, Wang Y, Johnson S, Barrett AJ, Young NS. Cytogenetic abnormalities in paroxysmal nocturnal haemoglobinuria usually occur in haematopoietic cells that are glycosylphosphatidylinositol-anchored protein (GPI-AP) positive. *Br J Haematol* 2003;**123**:173–6.
18. Parlier V, Tiainen M, Beris P, Miescher PA, Knuutila S, Jotterand Bellomo M. Trisomy 8 detection in granulomonocytic, erythrocytic and megakaryocytic lineages by chromosomal in situ suppression hybridization in a case of refractory anaemia with ringed sideroblasts complicating the course of paroxysmal nocturnal haemoglobinuria. *Br J Haematol* 1992;**81**:296–304.
19. Longo L, Bessler M, Beris P, Swirsky D, Luzzatto L. Myelodysplasia in a patient with pre-existing paroxysmal nocturnal haemoglobinuria: a clonal disease originating from within a clonal disease. *Br J Haematol* 1994;**87**:401–3.
20. Yue G, Hao S, Fadare O, Baker S, Pozdnyakova O, Galili N, Woda BA, Raza A, Wang SA. Hypocellularity in myelodysplastic syndrome is an independent factor which predicts a favorable outcome. *Leuk Res* 2008;**32**:553–8.
21. International Standing Committee on Human Cytogenetic Nomenclature, Shaffer LG, Slovak ML, Campbell LJ. *ISCN 2009: An International System for Human Cytogenetic Nomenclature*. Basel; Unionville, CT: Karger, 2009.
22. Cheson BD, Greenberg PL, Bennett JM, *et al.* Clinical application and proposal for modification of the International Working Group (IWG) response criteria in myelodysplasia. *Blood* 2006;**108**:419–25.
23. Camitta BM, Doney K. Immunosuppressive therapy for aplastic anemia: indications, agents, mechanisms, and results. *Am J Pediatr Hematol Oncol* 1990;**12**:411–24.
24. Sugimori C, Chuhjo T, Feng X, Yamazaki H, Takami A, Teramura M, Mizoguchi H, Omine M, Nakao S. Minor population of CD55-CD59- blood cells predicts response to immunosuppressive therapy and prognosis in patients with aplastic anemia. *Blood* 2006;**107**:1308–14.
25. Araten DJ, Nafa K, Pakdeesuwan K, Luzzatto L. Clonal populations of hematopoietic cells with paroxysmal nocturnal hemoglobinuria genotype and phenotype are present in normal individuals. *Proc Natl Acad Sci USA* 1999;**96**:5209–14.
26. Sugimori C, Mochizuki K, Qi Z, Sugimori N, Ishiyama K, Kondo Y, Yamazaki H, Takami A, Okumura H, Nakao S. Origin and fate of blood cells deficient in glycosylphosphatidylinositol-anchored protein among patients with bone marrow failure. *Br J Haematol* 2009;**147**:102–12.
27. Kulagin A, Golubovskaya I, Ganapiev A, *et al.* Prognostic value of minor PNH clones in aplastic anaemia patients treated with ATG-based immunosuppression: results of a two-centre prospective study. *Bone Marrow Transplant* 2011;**46**: S83–4.
28. Parker C, Omine M, Richards S, *et al.* Diagnosis and management of paroxysmal nocturnal hemoglobinuria. *Blood* 2005;**106**:3699–709.
29. Kanda Y. Investigation of the freely available easy-to-use software 'EZR' for medical statistics. *Bone Marrow Transplant* 2013;**48**:452–458.
30. Seiki Y, Sasaki Y, Hosokawa K, Saito C, Sugimori N, Yamazaki H, Takami A, Nakao S. Increased plasma thrombopoietin levels in patients with myelodysplastic syndrome: a reliable marker for a benign subset of bone marrow failure. *Haematologica* 2013;**98**:901–907.
31. Sloand EM, Pfannes L, Chen G, Shah S, Solomou EE, Barrett J, Young NS. CD34 cells from patients with trisomy 8 myelodysplastic syndrome (MDS) express early apoptotic markers but avoid programmed cell death by up-regulation of antiapoptotic proteins. *Blood* 2007;**109**:2399–405.
32. Katagiri T, Sato-Otsubo A, Kashiwase K, *et al.* Frequent loss of HLA alleles associated with copy number-neutral 6pLOH in acquired aplastic anemia. *Blood* 2011;**118**:6601–9.
33. Greenberg PL, Tuechler H, Schanz J, *et al.* Revised international prognostic scoring system for myelodysplastic syndromes. *Blood* 2012;**120**:2454–65.
34. Saumell S, Florensa L, Luno E, *et al.* Prognostic value of trisomy 8 as a single anomaly and the influence of additional cytogenetic aberrations in primary myelodysplastic syndromes. *Br J Haematol* 2012;**159**:311–21.

Supporting Information

Additional Supporting Information may be found in the online version of this article:

Figure S1. One patient who possessed 0.002% GPI-AP$^-$ granulocytes was judged positive because 0.026% of the patient's erythrocytes were GPI-AP$^-$ cells.

Figure S2. Changes in the proportion of +8 cells for six patients. The percentage of +8 clones revealed by G-banding increased in three patients (UPN3, 20, 33) and decreased in two patients (UPN2, 9) after successful IST.

© 2014 John Wiley & Sons A/S. Published by John Wiley & Sons Ltd

Biochemical Pharmacology 89 (2014) 361–369

Contents lists available at ScienceDirect

Biochemical Pharmacology

journal homepage: www.elsevier.com/locate/biochempharm

Constitutive activation of the ATM/BRCA1 pathway prevents DNA damage-induced apoptosis in 5-azacytidine-resistant cell lines

Satoshi Imanishi [a,*], Tomohiro Umezu [a,b], Kazushige Ohtsuki [a,c], Chiaki Kobayashi [c], Kazuma Ohyashiki [c], Junko H. Ohyashiki [a]

[a] Institute for Medical Science, Tokyo Medical University, 6-7-1 Nishi-shinjuku, Shinjuku, Tokyo 160-0023, Japan
[b] Department of Molecular Science, Tokyo Medical University, 6-7-1 Nishi-shinjuku, Shinjuku, Tokyo 160-0023, Japan
[c] First Department of Internal Medicine, Tokyo Medical University, 6-7-1 Nishi-shinjuku, Shinjuku, Tokyo 160-0023, Japan

ARTICLE INFO

Article history:
Received 27 January 2014
Accepted 17 March 2014
Available online 26 March 2014

Chemical compounds studied in this article:
5-Azacytidine (PubChem CID: 9444)
2-desoxy-5-azacytidine (PubChem CID: 451668)
3-deazauridine (PubChem CID: 3000824)
RG108 (PubChem CID: 702558)
caffeine (PubChem CID: 2519)
KU55933 (PubChem CID: 5278396)
mitomycin C (PubChem CID: 5746)
etoposide (PubChem CID: 36462)
cisplatin (PubChem CID: 441203)

Keywords:
5-Azacytidine
DNA demethylation
DNA damage

ABSTRACT

5-Azacytidine (AZA) exerts its anti-tumor effects by exerting cytotoxicity *via* its incorporation into RNA and DNA, which causes the reactivation of aberrantly silenced growth-regulatory genes by promoter demethylation, as well as DNA damage. AZA is used for patients with myelodysplastic syndrome and acute myeloid leukemia. However, some patients demonstrate resistance to AZA, the mechanisms of which are not fully elucidated. We therefore sought to better characterize the molecular mechanism of AZA resistance using an *in vitro* model of AZA resistance. We established AZA-resistant cell lines by exposing the human leukemia cell lines U937 and HL-60 to clinical concentrations of AZA, and characterized these cells. AZA-resistant cells showed a down-regulation of the DNMT3A protein, in correlation with their marked genome-wide DNA hypomethylation. Furthermore, genes involved in pyrimidine metabolism were down-regulated in both AZA-resistant cell lines; AZA sensitivity was restored by inhibition of CTP synthase. Of note is that the DNA damage response pathway is constitutively activated in the AZA-resistant cell lines, but not in the parental cell lines. Inhibition of the DNA damage response pathway canceled the AZA resistance, in association with an increase in apoptotic cells. We found that the molecular mechanism underlying AZA resistance involves pyrimidine metabolism and the DNA damage response through ATM kinase. This study therefore sheds light on the mechanisms underlying AZA resistance, and will enable better understanding of AZA resistance in patients undergoing AZA treatment.

© 2014 Elsevier Inc. All rights reserved.

1. Introduction

5-Azacytidine (AZA) is one of the most effective DNA demethylating agents used in cancer treatment. It is used for the treatment of patients with myelodysplastic syndromes (MDS) and acute myeloid leukemia (AML) in the USA, Europe, and Japan, among others, and yields a 40–60% response rate in these diseases [1]. However, some patients treated with AZA develop resistance against AZA after various treatment durations [2,3]. The prognosis of MDS patients after AZA treatment failure is poor, with a median overall survival time of 5.6 months [4].

AZA exerts its anti-tumor effects *via* its incorporation into RNA and DNA [5]. Induction of the differentiation of malignant cells might also be involved in the anti-tumor effects of AZA [6]. AZA taken up by cells is phosphorylated to azacytidine monophosphate (azaCMP) by uridine–cytidine kinase 2 (UCK2), and approximately 80–90% of azaCMP is subsequently phosphorylated to azacytidine triphosphate (azaCTP), which is incorporated into RNA. AzaCTP incorporated into RNA then promotes the degradation of RNA and inhibits protein synthesis [5].

Abbreviations: AZA, 5-azacytidine; MDS, myelodysplastic syndromes; AML, acute myeloid leukemia; azaCMP, azacytidine monophosphate; azaCTP, azacytidine triphosphate; DNMT, DNA methyltransferase; DAC, 2-desoxy-AZA; CDKN, cyclin dependent kinase inhibitor; TP53, tumor protein p53; PTEN, phosphatase and tensin homolog; WT1, Wilms tumor 1; RB1, retinoblastoma 1; POLR2B, polymerase (RNA) II (DNA directed) polypeptide B; UCK2, uridine–cytidine kinase 2; CDA, cytidine deaminase; AK3, adenylate kinase 3; POL II, RNA polymerase II; CTP, cytidine triphosphate; UTP, uridine triphosphate; 3-DU, 3-deazauridine; MMC, mitomycin C; phosphorylated proteins were indicated as, p-protein symbol.

* Corresponding author at: 6-7-1 Nishi-shinjuku, Shinjuku, Tokyo 160-0023, Japan. Tel.: +81 3 3342 6111; fax: +81 3 3345 0185.
E-mail address: s-ima@tokyo-med.ac.jp (S. Imanishi).

http://dx.doi.org/10.1016/j.bcp.2014.03.008
0006-2952/© 2014 Elsevier Inc. All rights reserved.

The remaining 10–20% of azaCMP is further mono-phosphorylated and converted to 2′-deoxy-azaCTP (aza-dCTP) by ribonucleotide reductase. Aza-dCTP is subsequently incorporated into DNA during replication [5]. When incorporated into a hemimethylated CpG site, the 2′-deoxy-azaCTP entraps DNA methyltransferase (DNMT) 1, whereas when it is incorporated into an unmethylated CpG site, it captures DNMT3A or DNMT3B [7], and forms covalent DNMT–DNA adducts. The formation of DNMT–DNA adducts induces the DNA damage response [8], subsequently resulting in cytotoxicity, and also causes the depletion of soluble DNMT protein levels, leading to replication-dependent global demethylation [9] and gene reactivation [10]. The DNA damage response induced by DNA damaging stimuli, as well as AZA [11], involves the activation of the Ataxia telangiectasia mutated (ATM) protein [12]. This is followed by phosphorylation and activation of checkpoint kinase 1 and 2 (CHK1 and CHK2) and breast cancer 1, early onset (BRCA1) proteins. Activated CHK1 and CHK2 phosphorylate p53 resulting in cell cycle arrest and apoptosis, whereas activated of BRCA1 promotes DNA damage repair [12].

The recent attention given to the activity of AZA or 2-desoxy-AZA (DAC) has focused on their demethylating activity rather than on their induction of DNA damage. Attention has particularly been given to demethylation in the promoter region of tumor-suppressor genes, because MDS and AML involve the abnormal regulation of epigenetic modifications [13,14]. The major obstacle toward the understanding of AZA sensitivity and resistance is that the degrees of involvement of each mechanism, namely, the incorporation of AZA into RNA, DNA, or both, in exerting the clinical and hematological improvements in MDS and AML are not yet fully elucidated.

To overcome this obstacle, we established cell lines that are resistant to clinical doses of AZA, from AZA-sensitive human leukemia cell lines, and compared their molecular and cellular properties to clarify the mechanism underlying AZA activity and resistance.

2. Materials and methods

2.1. Cell culture and reagent treatment

A human histiocytic leukemia cell line U937 [15], a human promyelocytic leukemia cell line HL-60 [16], and their AZA-resistant derivatives R-U937 and R-HL-60 cells were incubated in RPMI 1640 medium (Life Technologies Inc., Carlsbad, CA, USA) including 10% inactivated fetal bovine serum and 1% penicillin/streptomycin (Life Technologies). For the maintenance of R-U937 and R-HL-60 cells, AZA was added to the medium at a final concentration of 3 μM. For treatment with the reagents, cells were collected by centrifugation and resuspended at 3×10^5 cells/ml in fresh medium with the agents or the vehicle. For immunostaining and western blotting of proteins of the DNA damage response pathway, R-U937 and R-HL-60 cells were incubated in the absence of AZA for one week before the experiment. Cell viability was measured by the Cell Counting Kit-8 (Dojindo, Kumamoto, Japan), as reported previously [17]. Apoptotic cells were quantified using the FITC Annexin V Apoptosis Detection Kit I (BD Biosciences, Franklin Lakes, NJ, USA) as follows. Cells were treated with the indicated reagents for 36 h. After washing in ice-cold phosphate-buffered saline (PBS), the cells were incubated with FITC-labeled annexin V and propidium iodide (PI) for 15 min at room temperature in the dark. Flow cytometric measurements were performed on a BD Accuri C6 Flow Cytometer (BD Biosciences). A 488 nm blue laser was used for the excitation, and signals were detected by the FL1 channel (533 nm) for FITC and were detected by the FL2 channel (585 nm) for PI. The signals of 30,000 events were obtained. Analyses of the obtained data were performed using the C6 software Ver. 1.0 (BD Biosciences).

2.2. Chemical reagents and antibodies

The reagents used in this study were from the following sources. AZA, DAC, RG108, mitomycin C (MMC), etoposide (ETP) and cisplatin (CDDP) were purchased from Wako Pure Chemical Industries Ltd. (Osaka, Japan), and 3-deazauridine (3-DU) and caffeine were purchased from Sigma Aldrich Inc. (St. Louis, MO, USA). The ATM kinase inhibitor KU55933, the PARP inhibitor olaparib, the anti-DNMT1 antibody 4H80, the anti-DNMT3A antibody H-295, the anti-DNMT3B antibody Q-25, the anti-ATM antibody 2C1 and the anti-β-ACTIN antibody C4 were purchased from Santa Cruz Biotechnology Inc. (Dallas, TX, USA). The anti-phosphorylated H2AX (p-H2AX) antibody was purchased from Trevigen Inc. (Gaithersburg, MD, USA). The anti-phosphorylated ATM (Ser1981) (p-ATM) antibody 10H11.E12 was purchased from Upstate (Temecula, CA, USA). Antibodies for the phosphorylated form of p53 (Ser15) (p-p53), BRCA1 (Ser1524) (p-BRCA1), CHK1 (Ser345) (p-CHK1), CHK2 (Thr68) (p-CHK2), and ATR (Ser428) (p-ATR) were contained in the DNA Damage Antibody Sampler Kit purchased from Cell Signaling Technology Inc. (Danvers, MA, USA) and the anti-ATR antibody was purchased from Rockland Immunochemicals Inc. (Gilbertsville, PA, USA). Anti-P-glycoprotein antibody JSB-1 was purchased from Abcam Plc. (Cambridge, UK). The secondary antibodies, namely, horseradish peroxidase (HRP)-labeled anti-mouse IgG antibody and HRP-labeled anti-rabbit IgG antibody were purchased from GE Healthcare (Buckinghamshire, UK). Alexa 546-labeled anti-rabbit IgG antibody and Alexa 488-labeled anti-mouse IgG antibody were purchased from Life Technologies Inc.

2.3. Western blotting

Western blotting was performed as previously described [17]. Briefly, the membranes were probed with antibodies directed against DNMT1 (1:200), DNMT3A (1:200), DNMT3B (1:200), p-ATM (1:500), p-ATR (1:500), p-p53 (1:500), p-BRCA1 (1:500), p-CHK1 (1:500), p-CHK2 (1:500), ATM (1:200), ATR (1:500) or β-ACTIN (1:200) and then treated with the appropriate secondary antibodies. The amount of each protein was determined using the Image J software.

2.4. Methylation analysis

To determine the global DNA methylation levels, we performed the single-molecule methylation assay (SMMA) as previously described [18]. Briefly, TAMRA-labeled methyl-CpG-binding domain protein 2 (MBD2), unlabeled MBD2, 0% methylated DNA (negative control) and 100% methylated DNA (positive control) were used. Comprehensive analyses using the Infinium HumanMethylation450 BeadChip Kit (Illumina, San Diego, CA, USA) were also performed according to the manufacturer's instructions. Briefly, DNA samples were treated with bisulfite using the EZ DNA Methylation Kit (Zymo Research, CA, USA). The bisulfite-treated DNA was fragmented and suspended in hybridization buffer. The fragmented DNA was then dispensed onto a HumanMethylation450 BeadChip and hybridization was performed for 20 h. The methylation level of each CpG locus was calculated using the GenomeStudio Methylation Module (Illumina) as a methylation β-value (β = intensity of the methylated allele (M)/(intensity of the unmethylated allele (U) + intensity of the methylated allele (M) + 100). The heat maps were created using the GeneSpring 12.5 GX software (Agilent Technologies, Santa Clara, CA, USA) using the β-value without any modification. Analyses of the methylation levels in the promoter regions of specific genes were performed using the Methylated DNA

immunoprecipitation (MeDIP) assay kit (Active Motif, Carlsbad, CA, USA) following the manufacturer's instructions.

2.5. Quantitative RT-PCR

Quantitative RT-PCR was performed as previously described [19]. Taqman gene expression assays were used for *AK3* (Hs00750254_s1), *CDA* (Hs00156401_m1), *UCK2* (Hs00367072_m1) and *POLR2B* (Hs00265358_m1). The TaqMan Pre-Developed Assay Reagent (Life Technologies) was used for *ACTB*. The expression level of each gene relative to the expression level of *ACTB* was determined by the ΔCT method.

2.6. Immunocytochemistry

Cells were fixed in 4% formalin in PBS at 4 °C overnight. After washing and permeabilization in 0.1% TritonX-100 in PBS, cells were treated with an anti-p-H2AX antibody (1:500) or an anti-p-ATM antibody (1:200) at room temperature for 1 h, and then washed in PBS. After treatment with the appropriate secondary antibody, nuclei were stained with Hoechst 33342 (Dojindo, Kumamoto, Japan). The cells were then observed and photographed using the Biozero BZ-8100 fluorescence microscope system (Keyence, Osaka, Japan). For the analysis of p-H2AX-positive cells, 3 photographs of each sample, with each photograph including >200 cells, were analyzed using the Image J software. The ratio of p-H2AX-positive cells was determined as Alexa 546-positive cells/Hoechst positive nuclei.

2.7. Statistical analysis

For statistical analyses, one-way or two-way ANOVA followed by the *t*-test was performed using the GraphPad PRISM 6 software (GraphPad Software Inc., La Jolla, CA, USA). The means ± SD are shown in the figures.

3. Results

3.1. Growth inhibitory effect of AZA in AZA-resistant cell lines

To establish AZA-resistant human leukemia cell lines, U937 and HL-60 cells were incubated with gradually increasing doses of AZA, from 0.1 μM to 3 μM for 9 months and 3 months respectively. The surviving cells were strongly resistant to AZA (Fig. 1A), and were designated as AZA-resistant U937 (R-U937) cells and AZA-resistant HL-60 (R-HL-60) cells. These cells were also resistant to DAC (Fig. 1B), indicating that they acquired cross-resistance to DAC. The AZA-resistant phenotype of the R-U937 and R-HL-60 cells were maintained even after incubation in medium without AZA for 6 months (Fig. 1C). Both AZA-resistant cell lines demonstrated a lower proliferation rate than their parental cell lines (Fig. 1D). AZA treatment increased the ratio of annexin V-positive and PI-positive cells in U937 and HL-60 cells, but not in R-U937 and R-HL-60 cells (Fig. 2A and B), suggesting that AZA-treated U937 and HL-60 cells die from apoptosis. FACS analysis for the multi-drug transporter P-gp detected no significant difference in expression between the AZA-resistant cells and the parental cells (data not shown), indicating that the resistant phenotype of the AZA-resistant cells does not involve multi-drug resistance.

3.2. DNMT protein expression and DNA methylation in AZA-resistant cell lines

We next examined the protein expression levels of DNMT1, DNMT3A and DNMT3B in the AZA-resistant cell lines. Compared with their parental cells, the AZA-resistant cells had equivalent expression levels of DNMT1, whereas their DNMT3A levels were significantly reduced (Fig. 3A). DNMT3B was not detected in any of the cell lines (data not shown). The SMMA demonstrated that global DNA methylation levels were significantly reduced in the AZA-resistant cell lines compared with their parental cells (Fig. 3B).

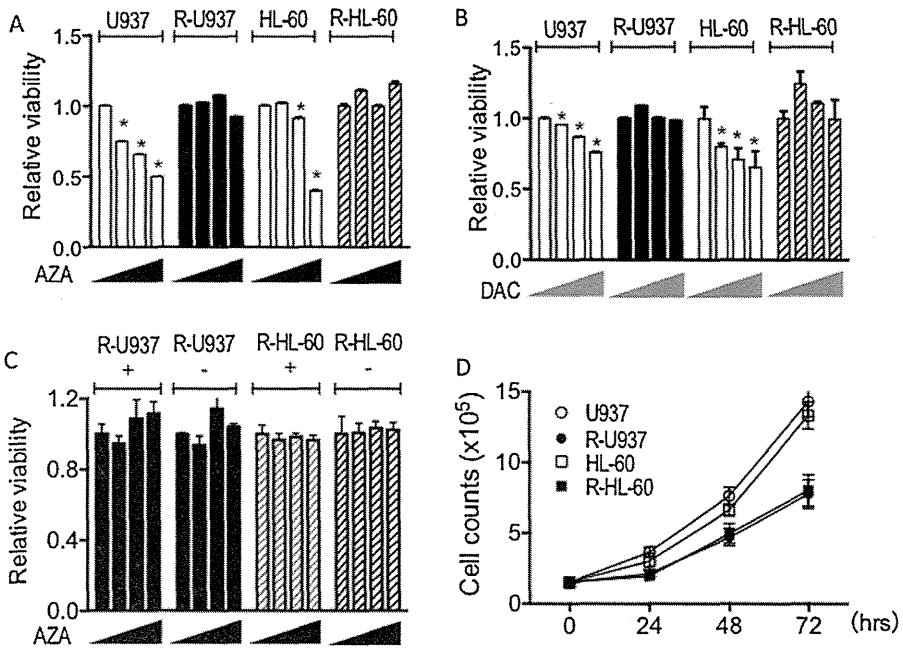

Fig. 1. Establishment of the AZA-resistant cell lines. (A, B) Viability of the cell lines in the presence of AZA (A) or DAC (B). R-U937 and R-HL-60 cells showed resistance to AZA and DAC. Each triangle indicates increasing doses, from left to right, of AZA (0, 1, 5 and 10 μM) or DAC (0, 0.2, 1 and 2 μM). *: $P < 0.01$ compared with cells in the absence of each reagent. (C) Comparison of AZA resistance of R-U937 and R-HL-60 cells after incubation with (+) or without (−) AZA for 6 months. The R-U937 and R-HL-60 cells were resistant to AZA even after incubation in medium without AZA for 6 months. Each triangle indicates increasing doses, from left to right, of AZA (0, 1, 5 and 10 μM). (D) Comparison of the cell growth between AZA-resistant cells and the parental cells. The AZA-resistant cell lines proliferated more slowly than their parental cells. The results from 3 independent experiments were analyzed.

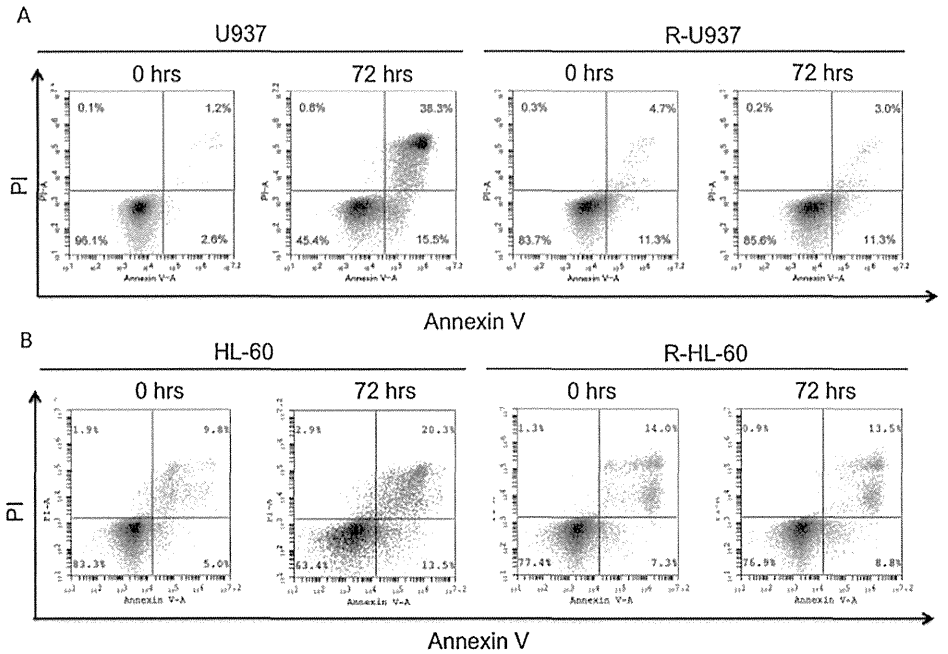

Fig. 2. FACS analyses of apoptosis of the cells in the presence of 10 μM AZA. (A, B) FACS analyses of U937 and R-U937 cells (A) and HL-60 and R-HL-60 cells (B) for annexin V and PI staining. The annexin V-positive and PI-positive fraction was increased in the parental cells but not in the AZA-resistant cells after 72 h of treatment with 10 μM of AZA. Typical plots from a representative experiment are shown. The experiments were repeated 3 times.

Global DNA demethylation was also confirmed by the methylation array (Fig. 3C). Furthermore, the DNA methylation array revealed a large variety of demethylation patterns among the tumor suppressor genes (Fig. 3D). For example, we found that most of the promoter regions of cyclin dependent kinase inhibitor 1A (*CDKN1A*) were demethylated in AZA-resistant cell lines compared with those in their parental cells, whereas the demethylation patterns of *CDKN1B*, *CDKN2A* and *CDKN2B* did not show a constant tendency. The promoter region of tumor protein p53 (*TP53*) was demethylated in both AZA-sensitive and AZA-resistant cells,

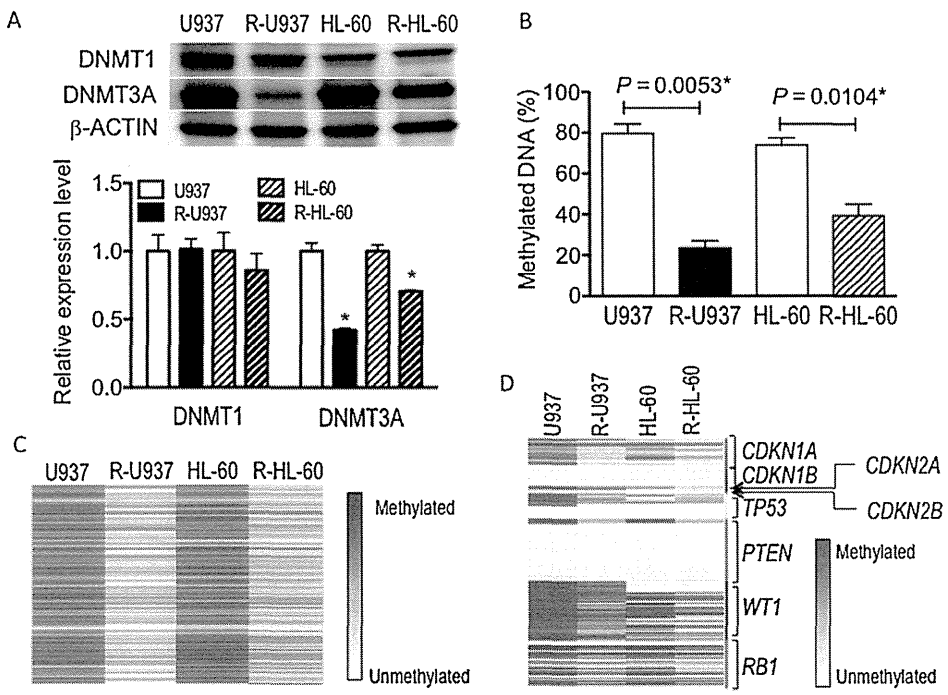

Fig. 3. DNMT protein expression and DNA methylation in AZA-resistant cells. (A) Protein levels of DNMT1 and DNMT3A. A decrease in the level of DNMT3A was evident in both AZA-resistant cell lines. The experiment was repeated 3 times. A representative blot is shown. The quantitative analyses are provided in the histogram. *: $P < 0.01$ compared with the parental cells. (B, C) Global DNA methylation was measured by the SMMA assay (B) and methylation array (C). Experiments were repeated 3 times for (B), and 2 times for (C). Methylation was significantly decreased in R-U937 and R-HL-60 cells compared with U937 and HL-60 cells. (D) DNA methylation patterns of various tumor suppressor genes.

whereas a part of the promoter regions of phosphatase and tensin homolog (*PTEN*) and Wilms tumor 1 (*WT1*) were demethylated in AZA-resistant cells. Demethylation in retinoblastoma 1 (*RB1*) was not prominent in the AZA-resistant cell lines.

3.3. Down-regulation of genes involved in the pyrimidine metabolism pathway in AZA-resistant cell lines

To investigate the biological relevance of the RNA-dependent pathway in AZA resistance, we first examined the RNA expression of genes involved in pyrimidine metabolism, such as polymerase (RNA) II (DNA directed) polypeptide B (*POLR2B*), uridine–cytidine kinase 2 (*UCK2*), cytidine deaminase (*CDA*), and adenylate kinase 3 (*AK3*), which were identified from the KEGG PATHWAY database (http://www.genome.jp/dbget-bin/www_bget?pathway:-map00240) [20,21]. We found that the RNA expression of *UCK2* and *POLR2B* was significantly decreased in both R-U937 and R-HL-60 cells compared with their parental cells (Fig. 4A and B), whereas the RNA expression of *AK3* and *CDA* was variable between the 2 cell lines. *POLR2B* encodes a rate-limiting subunit of RNA polymerase II (POL II) and *UCK2* encodes an enzyme specific for pyrimidine metabolism. These results indicate the biological relevance of *UCK2* and *POLR2B* in the AZA-resistant phenotype.

To determine whether altered pyrimidine metabolism results in a reduction of cytidine salvaging and acceleration of cytidine triphosphate (CTP) synthesis from uridine triphosphate (UTP), we incubated the AZA-resistant cell lines in 3-DU, a CTP synthase-specific inhibitor [22], with increasing doses of AZA. The viability of R-U937 and R-HL-60 cells was not affected by 40 μM and 5 μM 3-DU, respectively. AZA induced growth inhibition in a dose-dependent manner in the presence of 3-DU (Fig. 4C). Therefore, the accelerated conversion of UTP to CTP by CTP synthase plays an important role in AZA resistance.

To clarify the possible association between the down-regulation of genes involved in pyrimidine metabolism and the demethylation of their promoter region, we performed the MeDIP assay for the promoter regions of *UCK2* and *POLR2B*. Against our expectations, the promoter regions of these genes were highly demethylated in both the AZA-resistant cell lines and their parental cells, even when AZA was not added (Fig. 4D). We therefore could not find any AZA-induced demethylation in the AZA-resistant cell lines and their parental cells. These findings indicate that the down-regulation of genes involved in the RNA-dependent pathway is not due to demethylation of gene promoters by AZA.

3.4. Involvement of the DNA damage response pathway in AZA resistance

AZA is incorporated not only into RNA, but also into DNA, and inhibits DNMT activity. To clarify whether DNMT inhibition plays a central role in AZA sensitivity, we next compared the viability of the AZA-resistant cells and their parental cells in the presence or absence of RG108, which is a non-nucleoside analog DNMT inhibitor that does not damage DNA [23]. Since cell growth was not affected by RG108, we concluded that the growth-inhibitory effect of AZA might be due to DNA damage rather than DNMT inhibition (Fig. 5A). We then performed immunocytochemistry for phosphorylated H2AX (p-H2AX), which is a hallmark of the DNA damage response (Fig. 5B). U937 and HL-60 cells incubated with 10 μM AZA or 2 μM DAC showed a significantly higher ratio of p-H2AX-positive cells, whereas no such increase was detected in

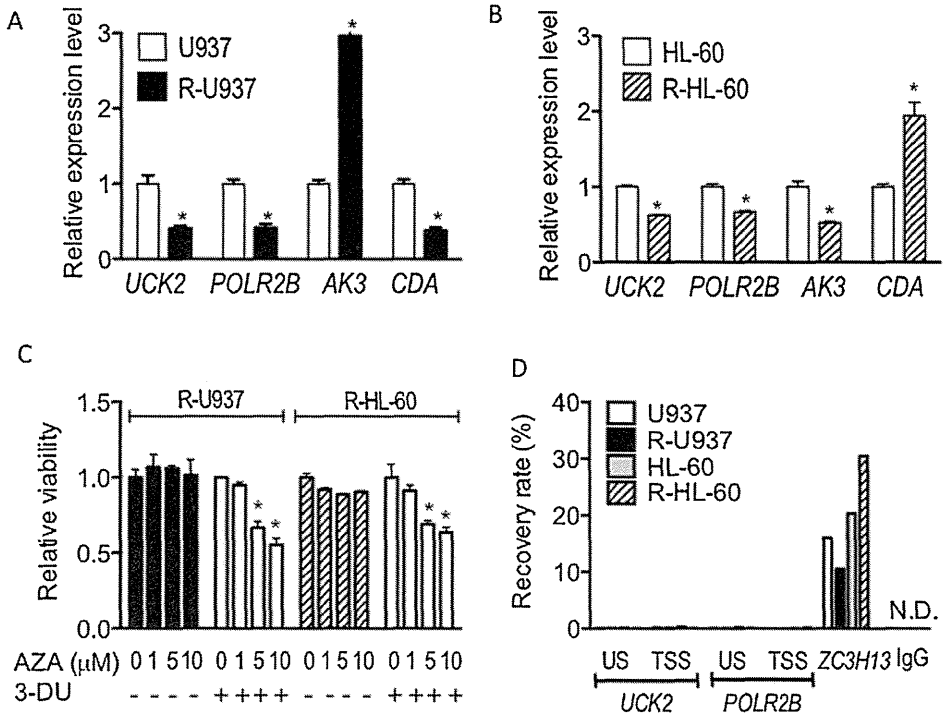

Fig. 4. Altered expression of genes involved in pyrimidine metabolism in AZA-resistant cells. (A, B) mRNA expression levels of pyrimidine metabolism genes in R-U937 (A) and R-HL-60 cells (B). The results from 3 independent experiments were analyzed. Means ± SD of relative mRNA expression levels normalized to *ACTB* are shown. The mRNA level in the parental cells was regarded as 1 for each gene. *: $P < 0.01$ compared with the mRNA expression level of each gene in the parental cells. (C) AZA reduced the viability of R-U937 and R-HL-60 cells in the presence of 3-DU. The results from 3 independent experiments were analyzed. *: $P < 0.01$ compared with the 3-DU-untreated control at each indicated dose. (D) Results of the MeDIP assay. The recovery rates for the transcription start site (TSS) and the area 500 bp upstream from the TSS (US) of *UCK2* and *POLR2B* are shown. Even in the absence of AZA, the AZA-resistant cells as well as their parental cells showed very low recovery rates in these regions. The results from 2 independent experiments were analyzed. A primer pair for *ZC3H13* was used as a positive control. IgG was used as a negative control for the anti-5-methylcytosine antibody. N.D., not detected.

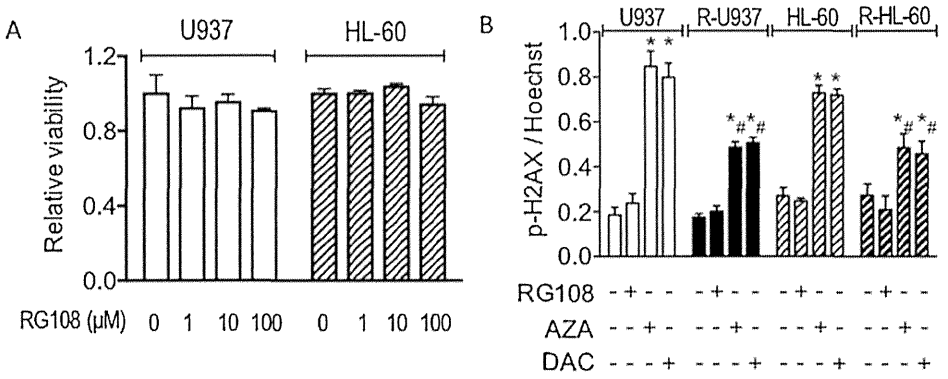

Fig. 5. DNA damage response in AZA-resistant cell lines. (A) Treatment with RG108 at the indicated doses did not reduce the viability of U937 and HL-60 cells. The results from 3 independent experiments were analyzed. (B) 10 μM AZA and 2 μM DAC increased the ratio of p-H2AX-positive cells in all the cell lines, whereas RG108 did not. *: $P < 0.01$ compared with the untreated control of each cell line. #: $P < 0.01$ compared with the parental cells treated with AZA or DAC. The results are shown as means ± SD.

U937 and HL-60 cells incubated with RG108. These results indicate that DNA damage plays a major role in exerting the effects of AZA and DAC on human leukemia cells. We also found that the ratio of p-H2AX-positive cells was increased in R-U937 and R-HL-60 cells exposed to AZA or DAC, although the increase was significantly lower in the AZA-resistant cells than in the parental cells.

To further elucidate the machinery associated with DNA damage, we stained phosphorylated ATM (p-ATM) in the AZA-resistant cells and their parental cells. In U937 and HL-60 cells, p-ATM-positive nuclear foci were not detected before AZA treatment, whereas p-ATM-positive nuclear foci were detected in the cells after AZA treatment (Fig. 6A). Unlike the parental cells, R-U937 and R-HL-60 cells already had a few p-ATM positive foci before AZA treatment, and the number of foci increased after AZA treatment. To clarify the role of the DNA damage response in AZA resistance, we compared the phosphorylation levels of the proteins involved in the DNA damage response, that is, ATM, Ataxia telangiectasia and Rad3 related (ATR), BRCA1, CHK1, CHK2 and p53, in U937 and R-U937 cells at 6, 24 and 48 h in the presence of 10 μM AZA, as well as before the treatment (Mock) (Figs. 6B and 7). In U937 cells in the presence of AZA, a significant increase in the phosphorylation of ATM and BRCA1 was detected at 6 h, and phosphorylation of CHK1, CHK2 and p53 was increased at 24 and 48 h. In R-U937 cells, ATM and BRCA1 were highly phosphorylated even in the absence of AZA, and their phosphorylation levels were further increased at 6 h and 24 h, respectively, in the presence of AZA. Phosphorylation of p53 and CHK2 was not increased even in the presence of AZA in R-U937 cells. Although phosphorylated CHK1 was significantly increased in R-U937 cells at 6 and 24 h, it was decreased to the basal level at 48 h. We were unable to detect the phosphorylated ATR protein (data not shown).

We then evaluated cell viability with or without caffeine, which is known to inhibit the DNA damage response pathway, with increasing doses of AZA or DAC. Eventually, we found that 1 mM caffeine reduced the viability of R-U937 and R-HL-60 cells in 10 μM of AZA or 2 μM of DAC (Fig. 8A). Although caffeine can

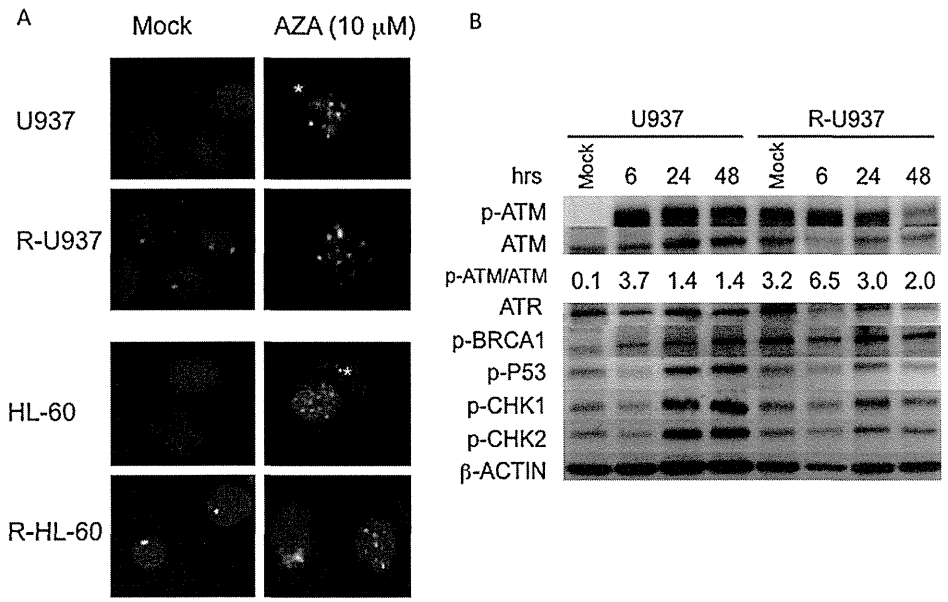

Fig. 6. ATM signaling plays roles in the acquisition of AZA resistance. (A) Immunostaining for p-ATM (Ser1981). Positive foci were observed in the nuclei of AZA-treated cells (right column). R-U937 and R-HL-60 possessed a few positive foci even in the absence of AZA (left column). Green: p-ATM (Ser1981). Blue: DAPI. *: Non-specific staining of dead cells. (B) Results of Western blotting for the phosphorylated proteins involved in the DNA damage response, p-ATM (Ser1981), p-p53 (Ser15), p-BRCA1 (Ser1524), p-CHK1 (Ser345), and p-CHK2 (Thr68), at the indicated times in the presence of 10 μM AZA. Typical photographs obtained from 3 independent experiments for each protein are shown. (For interpretation of the references to color in this figure legend, the reader is referred to the web version of this article.)

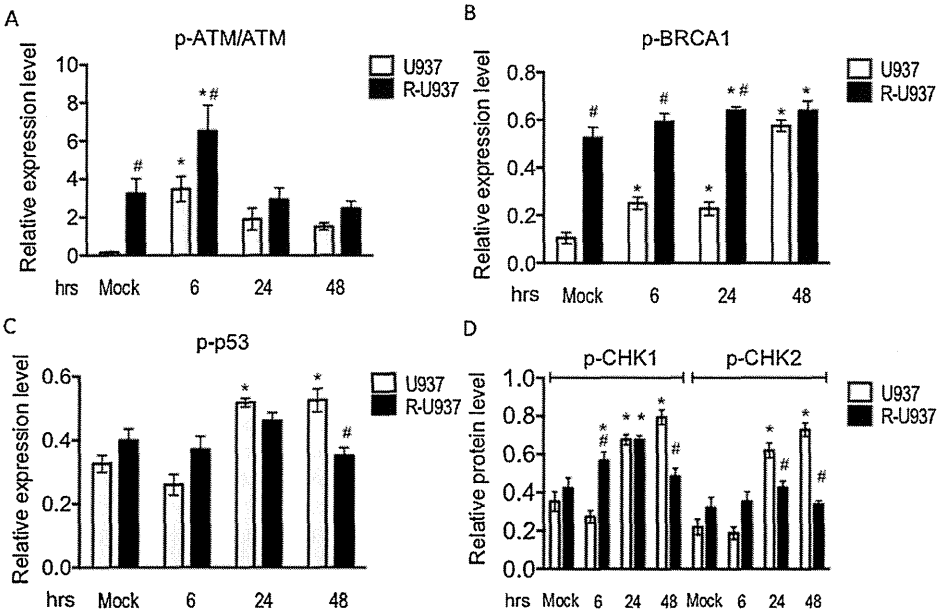

Fig. 7. Relative amounts of phosphorylated proteins of the DNA damage response pathway in U937 cells and R-U937 cells. Relative amount of p-ATM (Ser1981) (A), p-BRCA1 (Ser1524) (B), p-p53 (Ser15) (C), p-CHK1 (Ser345) and p-CHK2 (Thr68) (D) was quantified based on photographs obtained from 3 independent Western blotting experiments. The amount of p-ATM (Ser1981) was normalized to the amount of total ATM, and the others were normalized to the amount of β-ACTIN. *: $P < 0.05$ compared with the mock control. #: $P < 0.05$ compared with U937 cells of the corresponding hours.

affect multiple pathways, 10 μM of the ATM kinase activity specific inhibitor KU55933 also canceled the AZA resistance in R-U937 and R-HL-60 cells (Fig. 8A), demonstrating the critical role of the ATM-dependent DNA damage response pathway in the AZA resistance. Finally, to confirm the resistance to DNA damage of the AZA-resistant cell lines, we treated the cells with the DNA synthesis inhibitor MMC, the topoisomerase II inhibitor ETP, and the cross-linking agent CDDP. Although the susceptibility to these drugs greatly differed between the two parental cell lines, the AZA-resistant cell lines demonstrated higher resistance to the drugs than their corresponding parental cell lines (Fig. 8B and C).

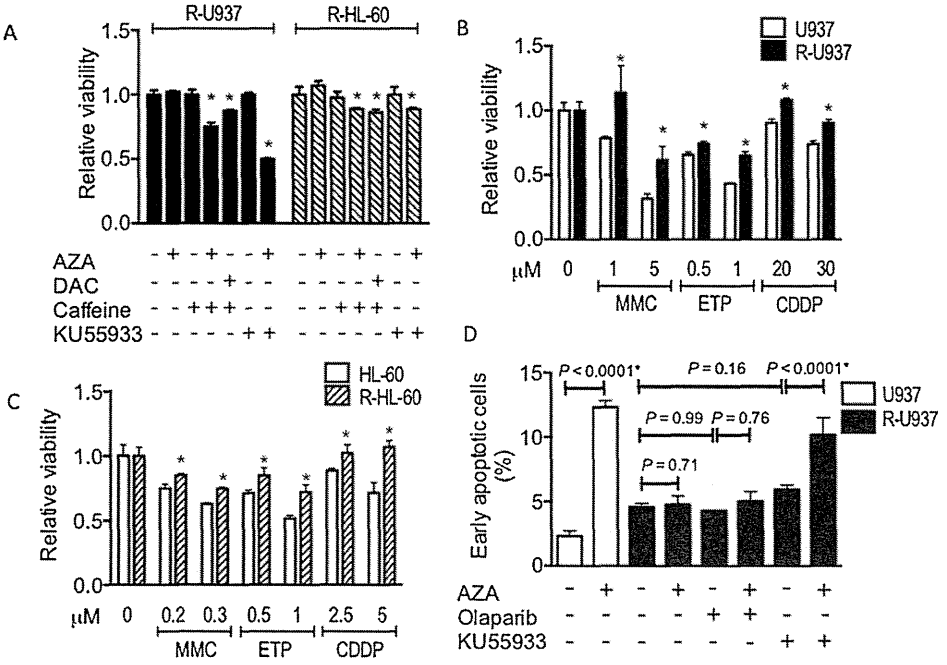

Fig. 8. Inhibition of the DNA damage response restores AZA sensitivity in AZA-resistant cells. (A) Caffeine and KU55933 canceled the AZA resistance of R-U937 and R-HL-60 cells, and caffeine canceled the DAC resistance of R-U937 and R-HL-60 cells. (B, C) Higher viabilities were detected in R-U937 (B) and R-HL-60 cells (C) than in their parental cells in the presence of mitomycin C (MMC), etoposide (ETP) and cisplatin (CDDP). *: The results from 3 independent experiments were analyzed for each graph. $P < 0.01$ compared with the parental cell line treated with the indicated dose of MMC, ETP or CDDP. The statistical analysis for each agent was performed independently. (D) Annexin V-positive cells were significantly increased in AZA-treated R-U937 cells in the presence of KU55933 compared with those in AZA-treated R-U937 cells in the absence of KU66933. In contrast, olaparib did not affect the percentage of annexin V-positive cells in the AZA-treated R-U937 cells.